Università degli Studi di Salerno
FACOLTÀ DI SCIENZE MATEMATICHE, FISICHE E NATURALI
Dipartimento di Fisica "E.R. Caianiello"

Tesi di Dottorato di Ricerca in Fisica
X Ciclo - Nuova Serie

Electric Transport Properties of S/F Hybrids: Weak and Inhomogenous Ferromagnet

Katsiaryna Ilyina

Advisor:

Prof. Carmine Attanasio
Università degli Studi di Salerno

Contents

Introduction

Superconductivity (S) and ferromagnetism (F) are competing phases whose coexistence is unlikely to occur. Exceptions require a non−uniform profile both for the pairing and the magnetization, as in the case of the FFLO state predicted independently by Fulde and Ferrell [1] and by Larkin and Ovchinnikov [2]. The coexistence of a superconducting and magnetic phase in a finite temperature range was first discovered in ternary rare earth compounds [3, 4]. Later on, other examples of coexistence of S and magnetic ordering were found [5–7] which motivated the investigation of alternative possibilities for the interplay of ferromagnetic and homogeneous superconducting order [8, 9]. Differently from the case of bulk systems, the coexistence may be easily achieved in artificial S/F hybrids, where the two antagonistic orderings are confined in spatially separated layers interacting via the proximity effect. Recently, these systems have been the subject of intensive theoretical and experimental studies and new concepts have been developed [10–14]. The improvement of the fabrication techniques has made possible the realization of heterostructures consisting of very thin layers of different materials coupled through high quality contacts. In this way, the reciprocal influence of the two opposite phases can be tuned by changing the materials, the layer thicknesses, and their configuration and topology. The analogy with the bulk situation is provided by the proximity effect: when a superconductor and a ferromagnet are brought into contact, Cooper pairs enter the F side and magnetic excitations leak into the S region across the S/F interface. As a result, superconductivity is suppressed in the superconductor within a distance ξ_S (the coherence length) from the interface, while S correlations are induced in the ferromagnet. The presence of the exchange field E_{ex} in F causes an energy shift between the electrons of the pairs entering in the ferromagnet and this results in the creation of Cooper pairs with non−zero momentum. Thus, the S order parameter does not simply decay in the F metal, as it would happen in a normal one, but it also oscillates in the direction perpendicular to the interface over a length scale given by ξ_F, the coherence length in F. This inhomogeneity of the order parameter may be interpreted as a manifestation of a FFLO phase in these structures [14–16].

In particular, in S/F hybrids, the inhomogeneous character of the S order param-

eter, caused by the proximity to the F side, leads to a non-monotonic behavior of all the physical quantities depending on the gap, as for instance for the transition temperature as a function of the F layer thickness, d_F [17]. In addition, re−entrant superconductivity has recently been experimentally observed as a function of d_F in Nb/CuNi bilayers [18, 19], as well as non-monotonic behavior of the anisotropy coefficient in S/F/S trilayers [20], negative critical current and reversed density of states in Josephson [21, 22] and tunnel [23] S/F/S π−junctions. Some peculiarities of the shape of the $R(T)$ curves in S/F/S trilayers and multilayers have been analyzed and, in general, transport properties of these systems have been studied [24–28]. Very recently, experimental results were obtained on S/F structures when measuring the dynamic instabilities of the vortex lattice at high driving currents. The role played on the non-equilibrium properties of the hybrids by both the ferromagnetic and the superconducting materials has been analyzed with a special focus on the values and the temperature dependence of the quasiparticle relaxation times, τ_E. Knowledge of the relaxation mechanisms in these systems is extremely important in view of possible applications since it can drive the optimal choice of both materials to realize, in particular, ultrafast superconducting single photon detectors based on S/F hybrid structures [29].

Another area of special interest in the field of the S/F structures concerns the investigation of spin triplet superconductivity [12]. In systems where the magnetization is spatially inhomogeneous, an equal spin pairing S component can be generated, that may survive over very long distances − of the order of the normal coherence length − inside F. In conventional spin−singlet S/F hybrids, superconductivity rapidly decays in the ferromagnet over distances of order of tenth of nanometers. However, the removal of the translational invariance due to the presence of interfaces leads, in clean systems, to a different mixed parity pairing, which can be responsible for the generation and the induction in the F side of a p−type spin−triplet component [30]. Such component can be induced in fully spin-polarized metals (half−metals) only in the presence of spin−active interfaces [31]. Recently it has been argued that in dirty systems even s−type spin−triplet superconductivity can survive in F over much longer distances [12, 32, 33]. Inhomogeneous magnetization in the F side [32, 33] or spin−active interfaces [34] can be responsible for the appearance of this triplet component. Some hints of the presence of odd−frequency spin−triplet correlations have been observed in S/F systems with half−metallic CrO_2 [35, 36], metallic Co−PdNi−CuNi layers [37] and more exotic Ho ferromagnet [38, 39].

In this work we will analyze the effect of different ferromagnets on the superconducting transport properties of S/F hybrids. In particular, in chapter 1 and chapter 2 weak ferromagnets such as PdNi and CuNi will be used in conjunction with Nb to study the static and dynamic properties of the vortex lattice in Nb/PdNi and Nb/CuNi bilayers to obtain information on the quasiparticles relaxation processes in these sys-

tems. The last two chapters of the thesis will be dedicated to the influence of the inhomogeneous magnetization present in thick Py layers on the upper critical fields and critical temperature in Nb/Py/Nb trilayers.

Bibliography

[1] P. Fulde and R. A. Ferrell, Phys. Rev. **135**, A550 (1964).

[2] A. I. Larkin and Yu. N. Ovchinnikov, Zh. Eksp. Teor. Fiz. **47** 1136 (1964); translation: Sov. Phys. JETP **20** 762 (1965).

[3] W. A. Fertig, J. K. Bachtacharjee, A. Bagchi, Phys. Rev. Lett. **38**, 987 (1977).

[4] D. E. Moncton, D. B. McWhan, P. H. Schmidt et al., Phys. Rev. Lett. **45**, 2060 (1980).

[5] L. Bauernfeind, W. Widder, and H. F. Braun, Physica C **254**, 151 (1995).

[6] S. S. Saxena, P. Agarwal, K. Ahilan,. F. M. Grosche, R. K. W. Haselwimmer, M. J. Steiner et al. Nature **406** 587 (2000).

[7] D. Aoki, A. Huxley, E. Ressouche, D. Braithwaite, J. Flouquet, J.-P. Brison, E. Lhotel, and C. Paulsen, Nature **413** 613 (2001).

[8] M. Cuoco, Phys.Rev.Lett. **91**, 197003-1 (2003).

[9] M. Cuoco, P. Gentile and C. Noce, Phys.Rev.B **68**, 054521 (2003).

[10] A. A. Golubov, M. Y. Kupriyanov, and E. Il'ichev, Rev. Mod. Phys. **76**, 411 (2004).

[11] A. I. Buzdin, Rev. Mod. Phys. 77, 935 (2005).

[12] F. S. Bergeret, A. F. Volkov, and K. B. Efetov, Rev. Mod. Phys. **77**, 1321 (2005).

[13] I. F. Lyuksyutov, V. L. Pokrovsky, Adv. Phys. **54** 67 (2005).

[14] Yu. A. Izyumov, Yu. N. Proshin, and M.G. Khusainov, Physics Uspekhi **45**, 109 (2002).

[15] M. Krawiec, B.L. Gyorffy and J.F. Annett, Phys.Rev.B **66**, 172505 (2002).

[16] E. A. Demler, G. B. Arnold, and M. R. Beasley, Phys.Rev.B 55, 15174 (1997).

[17] I. A. Garifullin, J. Magn.Magn.Mat. 240, 571 (2002).

[18] V. Zdravkov, A. Sidorenko, G. Obermeier, S. Gsell, M. Schreck,. C. Muller, S. Horn, R. Tidecks, and L. R. Tagirov, Phys.Rev.Lett. **97**, 057004 (2006).

[19] A. S. Sidorenko, V. I. Zdravkov, J. Kehrle, C. Morari, G. Obermeier, S. Gsell, M. Schreck, C. Muller, M. Yu. Kupriyanov, V. V. Ryazanov, S. Horn, L. R. Tagirov, R. Tidecks, JETP Lett. **90**, 139 (2009).

[20] C. Cirillo, C. Bell, G. Iannone, S. L. Prischepa, J. Aarts, and C. Attanasio, Phys.Rev.B **80**, 094510 (2009).

[21] T. Kontos, M. Aprili, J. Lesueur, F. Gen'et, B. Stephanidis, R. Boursier, Phys.Rev.Lett. **89**, 137007 (2002).

[22] V. V. Ryazanov, V. A. Oboznov, A. Yu. Rusanov, A. V. Veretennikov, A. A. Golubov, and J. Aarts, Phys.Rev.Lett. **86**, 2427 (2001).

[23] T. Kontos, M. Aprili, J. Lesueur, and X. Grison, Phys. Rev. Lett. **86**, 304 (2001).

[24] S. L. Prischepa, C. Cirillo, C. Bell, V. N. Kushnir, J. Aarts, C. Attanasio, M. Yu. Kupriyanov, ETP Lett. **88**, 375 (2008).

[25] C. Cirillo, S. L. Prischepa, M. Salvato, C. Attanasio, M. Hesselberth, J. Aarts, Phys.Rev. B **72**, 144511 (2005).

[26] G. Iannone, D. Zola, A. Angrisani Armenio, M. Polichetti, and C. Attanasio, Phys.Rev. B **75**, 064409 (2007).

[27] C. Cirillo, A. Rusanov, C. Bell, J. Aarts, Phys. Rev. B **75**, 174510 (2007).

[28] A. Angrisani Armenio, C. Cirillo, G. Iannone, S. L. Prischepa, and C. Attanasio, Phys. Rev. B **76**, 24515 (2007).

[29] C. Attanasio and C. Cirillo, J. Phys.: Condens. Matter **24** 083201 (2012).

[30] G. Annunziata, M. Cuoco, C. Noce, A. Romano, and P. Gentile, Phys.Rev.B **80**, 012503 (2009).

[31] M. Eschrig, J. Kopu, J. C. Cuevas, G. Schon, Phys. Rev. Lett. **90**, 137003 (2003).

[32] A. Kadigrobov, R. I. Shekhter, M. Jonson, Europhys. Lett. **54**, 394 (2001).

[33] A. F. Volkov, Ya. V. Fominov, and K. B. Efetov, Phys.Rev.B **72**, 184504 (2005).

[34] M. Eschrig and T. Lofwander, Nature Physics **4**, 138 (2008).

[35] R. S. Keizer, S. T. B. Goennenwein, T. M. Klapwijk, G. Miao, G. Xiao and A. Gupta, Nature **439**, 825 (2006).

[36] M. S. Anwar, F. Czeschka, M. Hesselberth, M. Porcu, and J. Aarts, Phys. Rev. B **82**, 100501 (2010).

[37] T. S. Khaire, M. A. Khasawneh, W. P. Pratt, Jr., and N. O. Birge, Phys. Rev. Lett. **104**, 137002 (2010).

[38] I. Sosnin, H. Cho, V. T. Petrashov, A. F. Volkov, Phys.Rev.Lett. **96**, 157002 (2006)

[39] J. W. A. Robinson, J. D. S. Witt, and M. G. Blamire, Science **329**, 59 (2010).

Chapter 1

Static and dynamic properties of the vortex lattice in Nb/PdNi bilayers

By measuring I−V characteristics as a function of the temperature and the external magnetic field, we have analyzed the static and dynamic properties of the vortex lattice in Nb/$Pd_{0.84}Ni_{0.16}$ bilayers. In particular, the critical current density J_c for the onset of the vortex motion and the dynamic instability of the moving vortex lattice at high driving currents have been studied and compared to the results obtained in a single Nb film. We find that J_c is smaller in the bilayers than in the single superconducting film due to the smaller value of the superconducting order parameter in the bilayers. The critical velocity v^* for the occurrence of the instability is larger in the S/F bilayers than in the single S layer. However, the quasiparticle energy relaxation rate extracted from v^* is almost temperature−independent, implying that a different relaxation mechanism plays a role in the Nb/$Pd_{0.84}Ni_{0.16}$ bilayers.

1.1 Introduction

Conventional singlet superconductivity (S) and ferromagnetism (F) are two competitive orderings which can coexist in artificial S/F hybrids interacting via the proximity effect [1]. Due to the spatial inhomogeneous nature of the order parameter induced in the F layer, many new effects have been recently observed such as, for example, the non-monotonic behavior of the superconducting critical temperature T_c

as a function of the F layer thickness, d_F, in many S/F heterostructures [2–4] or oscillations of the critical current in S/F/S Josephson junctions [5]. What essentially happens in these systems is that the presence of an exchange energy E_{ex} in F causes a momentum shift of the Cooper pairs entering the ferromagnet [6]. This implies that the superconducting order parameter does not simply decay in the ferromagnetic metal, as it happens in normal metals, but it oscillates perpendicularly to the F side of the interface over a distance ξ_F, the coherence length in the ferromagnet. In the dirty limit $\xi_F = \sqrt{\hbar D_F/E_{ex}}$ (D_F is the diffusion coefficient of the F metal) and this quantity should not be confused with the thermal diffusion length $\xi_F^* = \hbar D_F/2\pi k_B T_c$ [7]. In the case of weakly ferromagnetic alloys such as PdNi and CuNi these quantities are of the order of a few nanometers [8]. The nonhomogeneous character of the order parameter was also studied by measuring the depairing current density J_{dp} in Fe/Nb/Fe and Nb/$Pd_{0.81}Ni_{0.19}$ hybrids [9, 10] while the critical current density J_c together with the dynamic instability of the moving vortex lattice at high driving currents was investigated in superconducting Nb/$Ni_{0.80}Fe_{0.20}$ bilayers [11]. In the last case the strong ferromagnet (large E_{ex} and very small $\xi_F \approx 12$ nm) $Ni_{0.80}Fe_{0.20}$ (permalloy, Py) was used to strongly suppress the superconducting order parameter at the interface, confining it in the S layer, so that the effects of the inhomogeneous order parameter could be nicely investigated. In this Chapter we have studied, by measuring I−V curves, the static (connected to the onset of the vortex motion) and the dynamic (connected to the instability of the vortex lattice at high currents) properties of S/F bilayers. Nb has been chosen for the superconductor while a weakly ferromagnetic alloy (small E_{ex} and large ξ_F), $Pd_{0.84}Ni_{0.16}$, was chosen as the ferromagnetic metal. The measured critical currents J_c were smaller while the critical velocities v^* were larger than the corresponding quantities for the single Nb film as was observed in the case of Nb/Py [11]. Also, due to the weak magnetic strength of $Pd_{0.84}Ni_{0.16}$ with respect to Py, J_c was larger and v^* smaller than those measured in Nb/Py [11]. Moreover, the larger value of ξ_F in $Pd_{0.84}Ni_{0.16}$, seems to be responsible of the change of the quasiparticle relaxation mechanism in the Nb/$Pd_{0.84}Ni_{0.16}$ system. This Chapter is organized as follows. In section 1.2 we describe the sample fabrication, and the magnetic and electrical characterization of the weakly ferromagnetic alloy used in this work. Section 1.3 reports on the superconducting critical temperature measurements in Nb/$Pd_{0.84}Ni_{0.16}$ bilayers as a function of d_F. The theoretical fit to the experimental results allowed us to derive numbers for E_{ex} of the ferromagnet and for the transparency parameter γ_b of the interface contact in the S/F system. Finally, section 1.4 presents the main results of the Chapter, namely, critical currents and critical velocities of the Nb/$Pd_{0.84}Ni_{0.16}$ bilayer and their comparison to the values obtained in the case of a single Nb film and an Nb/Py bilayer [11].

1.2 Experimental details

1.2.1 Sample fabrication

Nb/$Pd_{0.84}Ni_{0.16}$ bilayers were grown on Si(100) substrates by UHV dc diode magnetron sputtering at an Ar pressure of 1×10^{-3} Torr after obtaining a base pressure of 2×10^{-3} Torr. The typical deposition rates were 0.28 nm s^{-1} for Nb and 0.40 nm s^{-1} for $Pd_{0.84}Ni_{0.16}$ measured by a quartz crystal monitor previously calibrated by low-angle x-ray reflectivity measurements on deliberately deposited thin films of each material. The Ni concentration in the $Pd_{0.84}Ni_{0.16}$ films was estimated by energy dispersion spectrometry analyses (EDS). The measurements revealed that the stoichiometry of the target (x = 0.10) was not conserved in the thin films, resulting in a higher Ni content, i.e. x = 0.16. The bilayer we used to study the static and dynamic properties of the vortex lattice had the same Nb and PdNi thickness: $d_{Nb} = d_{PdNi} = 30$ nm. The value for d_{PdNi} was chosen to be much greater than the $\xi_F \approx 3.3$ nm for our $Pd_{0.84}Ni_{0.16}$ (see section 1.2). Using a lift−off procedure samples were patterned into strips with width $w = 20$ μ m. The length between the voltage contacts was 300 μm. The critical temperature of this sample was $T_c = 6.3$ K. For comparison a 30 nm thick Nb film ($T_c = 7.3$ K) was also studied. To measure the I−V curves and the critical currents a standard four-probe technique has been used. In order to avoid possible heating effects the samples were put into direct contact with the liquid helium and the I−V characteristics were measured by using a pulsed technique. The current-on time was of 12 ms followed by a current-off time of 1 s. Any single voltage value was acquired at the maximum value of the current. This procedure was repeated by sweeping current upward and then downward and no hysteresis in the curves was detected, indicating that the instability detected in the I−V characteristics had no thermal origin. The magnetic field was applied perpendicular to both the plane of the substrate and the direction of the current. The temperature dependence of the perpendicular upper critical magnetic field $H_{c2\perp}(T)$ was resistively measured in the four-contact configuration; the values were extracted from the R(H) curves measured at constant temperature taking the 90% value of the normal state resistance R_N just above the transition to the superconducting state. From the slope of the perpendicular upper critical field the quasiparticle diffusion coefficient $D = (4k_B/\pi e)(-dH_{c2\perp}/dT|_{T=Tc})^{-1}$ has been estimated for the single Nb film [12]. Since the slope of the perpendicular upper critical field cannot be used to directly determine D for a layered system [11, 13, 14] the same value obtained for Nb, namely $D = 1.9 \times 10^{-4} m^2 s^{-1}$, has been used for calculations involving the Nb/PdNi bilayer. Single films of $Pd_{0.84}Ni_{0.16}$ were specially made in order

to study the electrical and magnetic properties of the ferromagnetic alloy. Finally, to investigate the dependence of the superconducting critical temperature T_c as a function of the ferromagnetic layer thickness d_F we deposited bilayers with constant Nb thickness $d_{Nb} = 15$ nm and variable thickness $d_{PdNi} = 0{-}10$ nm of $Pd_{0.84}Ni_{0.16}$. As we will show in much more detail in the following, the analysis of this curve allowed us to obtain information about the values of E_{ex} and the interface parameter γ_b.

1.2.2 Characterization of PdNi alloy

A number of preliminary characterizations were performed on single $Pd_{0.84}Ni_{0.16}$ films to obtain information about its transport and magnetic properties. Figure 1.1(a) shows the hysteresis loop of a single 50 nm thick $Pd_{0.84}Ni_{0.16}$ film performed using a SQUID magnetometer at $T = 10$ K with the surface of the sample parallel to the magnetic field. The value of the saturation magnetization at this temperature was $M_{sat} = 0.35\ \mu_B$/atom. For the same sample, the temperature dependence of the magnetic moment m was measured to derive the value of the Curie temperature, T_{Curie}. The sample was first magnetized to saturation at $T = 5$ K: the field was then removed and $m(T)$ was measured up to $T = 300$ K and down again to $T = 5$K. T_{Curie} was defined as the point where irreversibility appears when cooling down the sample, and was estimated to be $T_{Curie} = 190$ K, see figure 1.1(b).

Figure 1.2 shows the temperature dependence of the electrical resistance measured down to 100 K on the same single $Pd_{0.84}Ni_{0.16}$ film. Looking at the figure we can note the presence of a maximum followed by a decrease of the resistance when the temperature is lowered.

A connection to the magnetic properties of the sample can be done by looking at the behavior of the derivative of R with respect to T [15], $\mathrm{d}R/\mathrm{d}T$, which is plotted in the same graph (right scale). Defining T^R_{Curie} as the temperature where the curve starts to flatten [15], we estimate $T^R_{Curie} = 170$ K in reasonable agreement with the value obtained from magnetic measurements. The number we have obtained for the Curie temperature nicely fits into the overall dependence of T_{Curie} as a function of the Ni concentration as can be seen in figure 1.3 where this behavior is plotted using the data reported in the literature [10, 15–18].

In figure 1.4 the resistivity of $Pd_{0.84}Ni_{0.16}$ films measured at $T = 10$ K using the van der Pauw method is shown as a function of d_{PdNi}. The solid line represents the fit of the experimental data to the FuchsSondheimer formula [19]:

$$\rho = \rho_B(1 + 3l/8d_F) \tag{1.1}$$

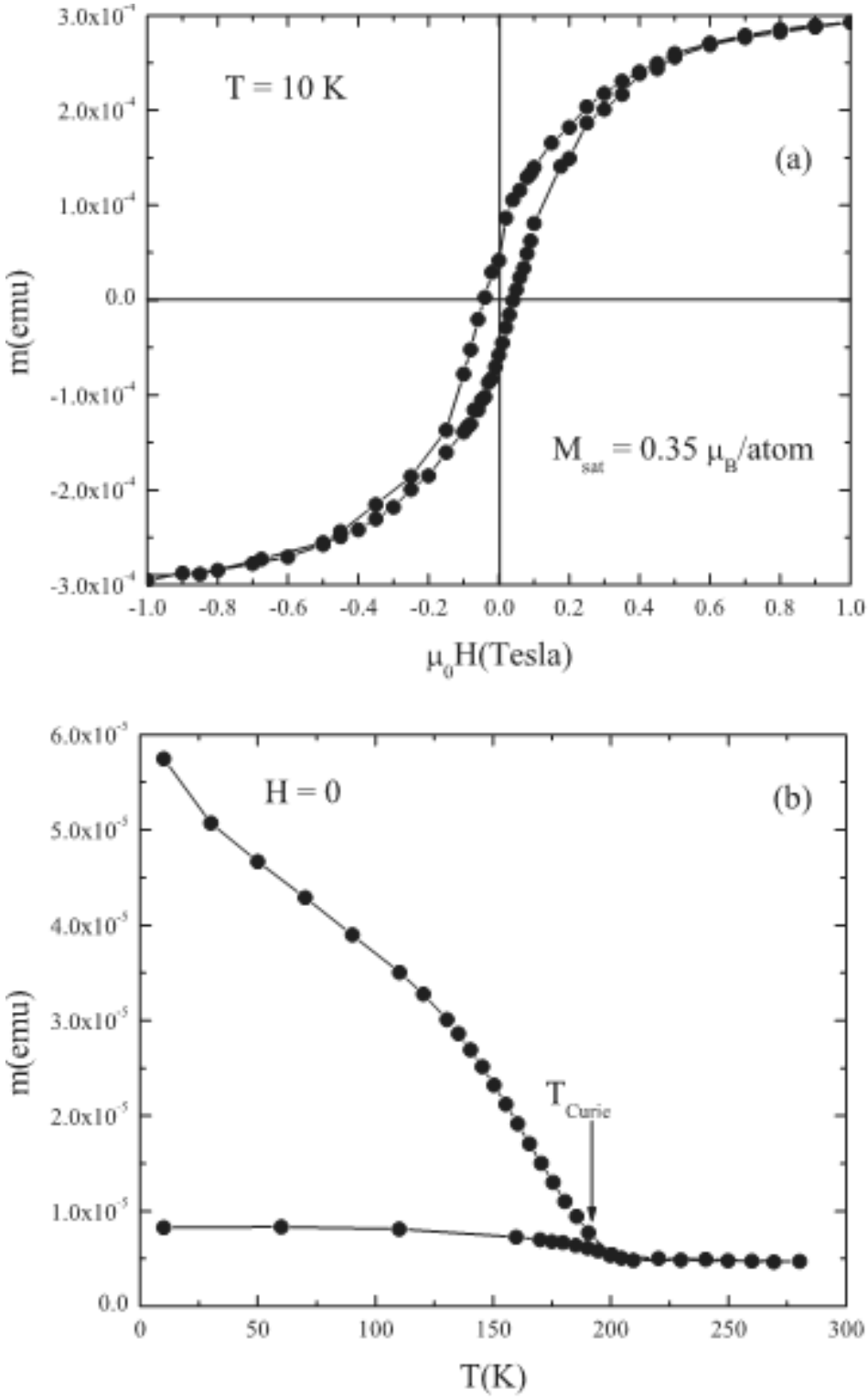

Figure 1.1: *(a) Magnetization loop for a 50 nm thick $Pd_{0.84}Ni_{0.16}$ film at $T = 10$ K. (b) Magnetic moment as a function of the temperature after saturation at $T = 5$ K measured for the same sample.*

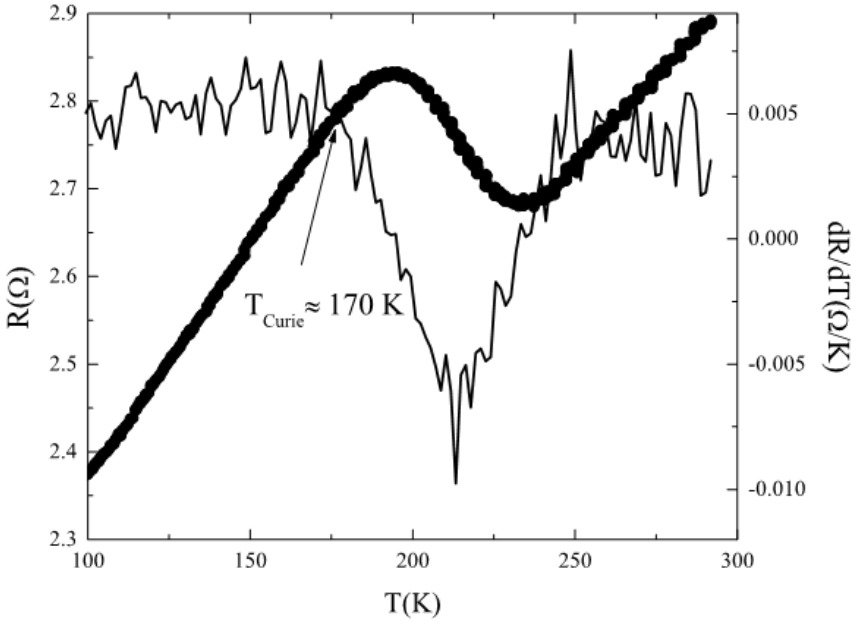

Figure 1.2: *Electrical resistance (left scale) and its first derivative (right scale) as a function of the temperature for the same 50 nm thick* $Pd_{0.84}Ni_{0.16}$ *film of figure 1.1.*

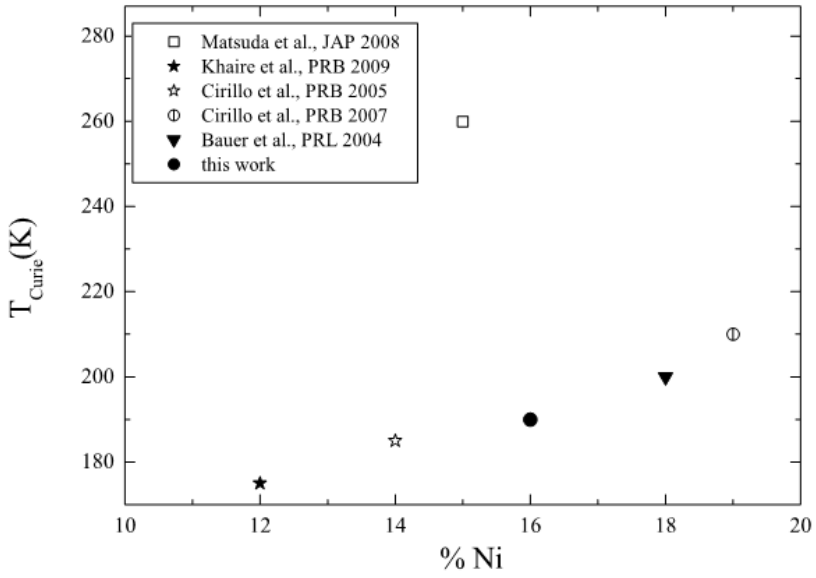

Figure 1.3: *Values for the Curie temperature for different values of the Ni concentration in the PdNi alloy. References to which the symbols refer are reported in the figure.*

where the two fitting parameters are ρ_B, the bulk resistivity, and l, the electronic mean free path in the ferromagnetic layer [20].

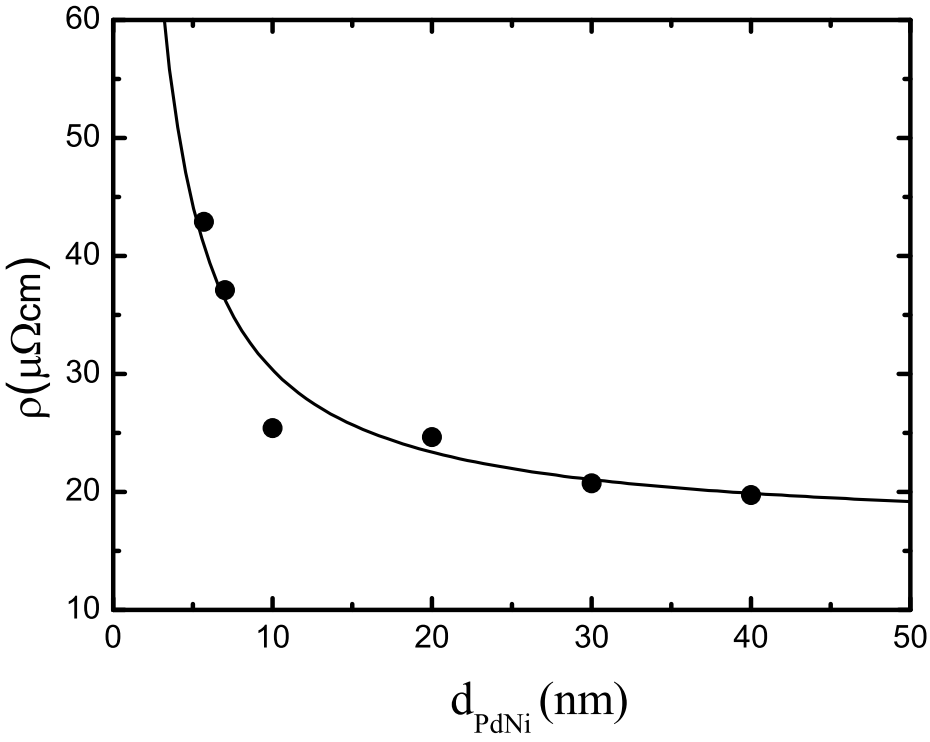

Figure 1.4: *Thickness dependence of the low temperature resistivity for* $Pd_{0.84}Ni_{0.16}$ *single films. The solid line is a fit to the experimental data obtained using equation 1.1.*

From the fitting procedure we obtain $\rho_B = 16.4\ \mu\Omega$ cm, which is a typical value for the low temperature resistivity for PdNi alloys with Ni concentrations similar to ours [11, 15]. We also obtain $l = 22$ nm. As is evident from figure 1.4, the low temperature resistivity drastically increases as the thickness is lowered below $d_F = 10$ nm. We will come back to this point in the following when we discuss the $T_c(d_F)$ fitting procedure.

1.3 Critical temperatures

Figure 1.5 shows the thickness dependence of the superconducting transition temperature for $Nb/Pd_{0.84}Ni_{0.16}$ bilayers with a constant value of d_{Nb}. Data were obtained from the R(T) curves measured using a four-probe configuration and the critical temperature was defined as the midpoint of the resistive transitions. It is clearly shown that T_c rapidly decreases with increasing the thickness of the ferromagnetic layer, reaching a shallow minimum around $d_{PdNi} \simeq 3.5$ nm.

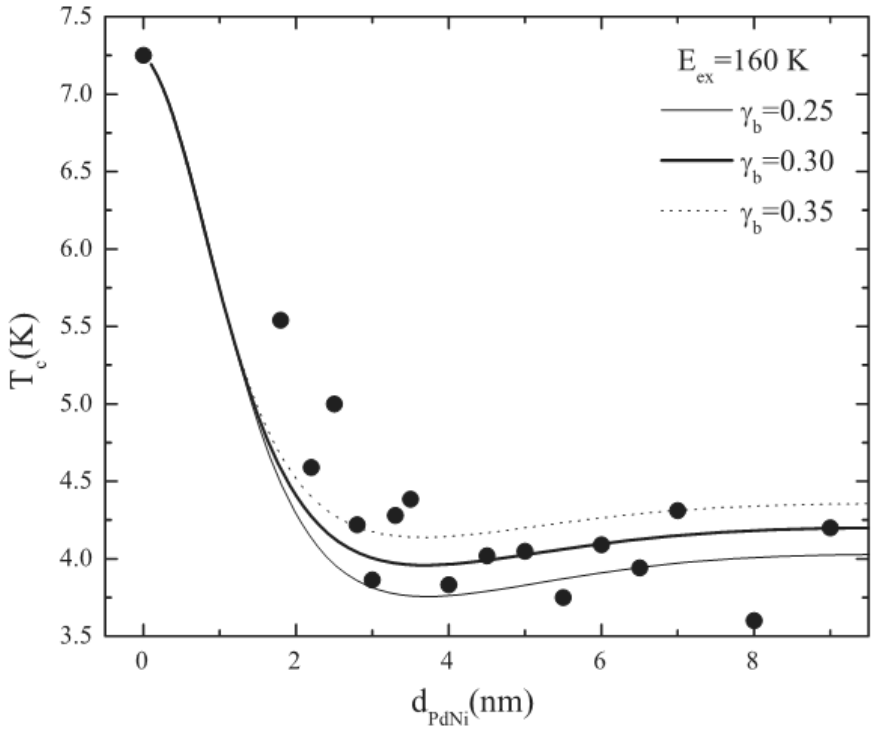

Figure 1.5: *The critical temperature, T_c, versus PdNi thickness, d_{PdNi}, in $Nb/Pd_{0.84}Ni_{0.16}$ bilayers. Different lines are the results of the theoretical fit in the single−mode approximation for different values of γ_b. See the text for details.*

This non−monotonic behavior of T_c was interpreted in the framework of the proximity effect theory proposed by Fominov et al in the limiting case known as the single-mode approximation [7]. In this model, which is valid in the dirty limit, the exchange energy inside the ferromagnetic metals is considered as the only pair-breaking mechanism. Moreover a finite transparency of the S/F contact is assumed. For more details regarding the formulae used for these calculations the reader can refer to [10, 15]. Here it is only worth remembering that all the microscopical parameters appearing in the equations have been estimated experimentally apart from E_{ex} and the parameter γ_b, the latter describing the effect of the boundary transparency $\mathcal{T}$, to which it is related by the relation:

$$\gamma_b = \frac{2}{3}\frac{l_F}{\xi_F^*}\frac{1-\mathcal{T}}{\mathcal{T}} \tag{1.2}$$

where $\mathcal{T}$ is zero for a completely reflecting interface and it is equal to one for a completely transparent contact [7, 22]. For a single Nb film, 15 nm thick, we measured a critical temperature $T_c = 7.25$ K, a low temperature resistivity $\rho_{Nb} = 25$ $\mu\Omega$ cm and, from the slope of the perpendicular upper critical field near T_c, a superconducting coherence length $\xi_{Nb} = 6.0$ nm. For the low temperature resistivity of the $Pd_{0.84}Ni_{0.16}$ layer, based on the dependence reported in figure we used $\rho_{PdNi} = 55$ $\mu\Omega$ cm. This value represents the resistivity of an single $Pd_{0.84}Ni_{0.16}$ film of about 3.5 nm, an intermediate thickness in the analyzed d_{PdNi} range. We also assumed a thickness−limited mean free path using an average value of $l_{PdNi} = 3.5$ nm. Using the Pd Fermi velocity $\upsilon_{Pd} = 2.00 \times 10^7$ cm s^{-1} [22, 23], this leads to a value of $\xi^*_{PdNi} = 6.2$ nm,being that $D_{PdNi} = \upsilon_{Pd} l_{PdNi}/3 = 2.3 \times 10^{-4}$ m^2 s^{-1}. In the simulation procedure, the γ_b value was determined from the vertical position of the $T_c(d_{PdNi})$ curve, while E_{ex} was selected to better reproduce the T_c saturation. A reasonable fit for $T_c(d_F)$ is obtained for $E_{ex} = 160$ K (≈ 14 meV) and $\gamma_b = 0.30$. The corresponding curve is shown as a solid line in figure 1.5. To demonstrate the sensitivity of the equations to γ_b, two more curves for different values of this parameter are also displayed, allowing us to estimate $\gamma_b = 0.30 \pm 0.05$. Regarding the value extracted for E_{ex}, this allows an estimation of $\xi_{PdNi} = \sqrt{\hbar D_{PdNi}/E_{ex}} = 3.3$ nm. This parameter is phenomenologically related to the position of the minimum in the $T_c(d_{PdNi})$ curve according to $d_{min} = 0.7\ \pi\xi_F/2$ [7]. With $d_{min} = 3.6$ nm, we find $\xi_{PdNi} = 3.2$ nm, in very good agreement with the previous value of ξ_{PdNi}. The fitting procedure enables us to estimate the value of the interface transparency of the $Nb/Pd_{0.84}Ni_{0.16}$ contact and, according to the expression 1.2, we obtain $\mathcal{T} \approx 0.55$. It also worth commenting on the disagreement between the theoretical fit and the experimental data for small d_{PdNi} values. Such a deviation, present in many works [7, 10, 24, 25], could be related to the fact that in this regime the microscopical parameters of the $Pd_{0.84}Ni_{0.16}$ layer strongly depend on the thickness, while in the model a unique value is used to describe the whole $T_c(d_{PdNi})$ dependence. Indeed, in this range the exchange energy as well as the mean free path strongly depend on the thickness. The discrepancy between the experimental data and the theoretical fit could be reduced by explicitly considering both E_{ex} and l_{PdNi} as thickness-dependent in the equations, but this is beyond the scope of this work. A final note concerns the values of the fitting parameters extracted from the simulation procedure, E_{ex} and γ_b. The value of the exchange energy scales with the ones obtained for Nb/PdNi systems for different Ni concentrations of the PdNi alloys. For the sake of completeness in figure 1.6 the dependence of E_{ex} on the Ni content in PdNi alloys, as extracted from the proximity effect, Josephson and tunnel experiments on Nb/PdNi systems taken from the literature, is reported [10, 15–18, 26–31]

The comparison between the different values extracted for γ_b, and consequently

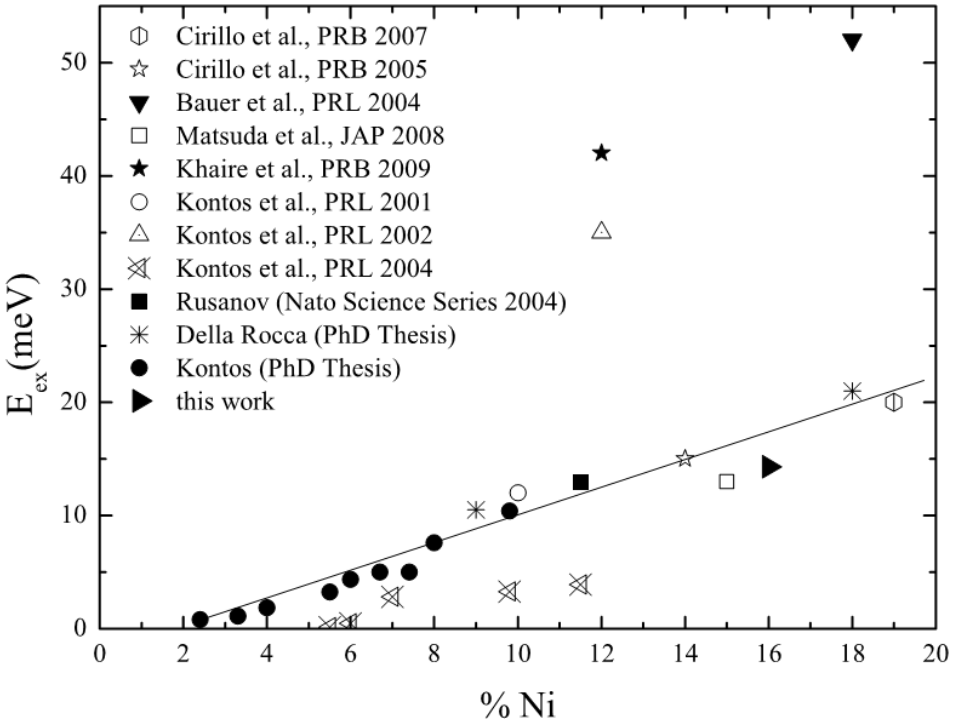

Figure 1.6: *Values for the exchange energy for different values of the Ni concentration in the PdNi alloy. References to which the symbols refer are reported in the figure.*

($\mathcal{T}$), appears to be more complicated as exhaustively reported in [15, 32]. If, on the one hand, the present result confirms the observation that the value of the interface transparency in superconducting/weakly ferromagnetic alloys is of the same order of magnitude as found in S/N systems [10, 15], it is also true that the quality of the interface dramatically depends on the different deposition conditions, or it could even be affected by different spin-flip scattering processes, which in the present theory are not taken into account.

1.4 Current−voltage characteristics

1.4.1 Critical currents

In figure 1.7(a) the I−V characteristics are shown for the single 30 nm thick Nb film at $T = 4.2$ K (t $\equiv T/T_c = 0.57$) for different values of the external magnetic field between 0.05 and 1.9 T, as indicated in the figure. The curves show a sudden jump at a well−defined current value I^*, well above the critical current I_c, where the onset of voltage due to the moving vortices starts to occur. At higher magnetic fields, the I−V curves become more smeared and finally the jump disappears. We will analyze this aspect in detail in the next paragraph. In figure 1.7(b), we show the I−V curves measured at $T = 3.6$ K (again $t = 0.56$) for the $Nb/Pd_{0.84}Ni_{0.16}$ bilayer.

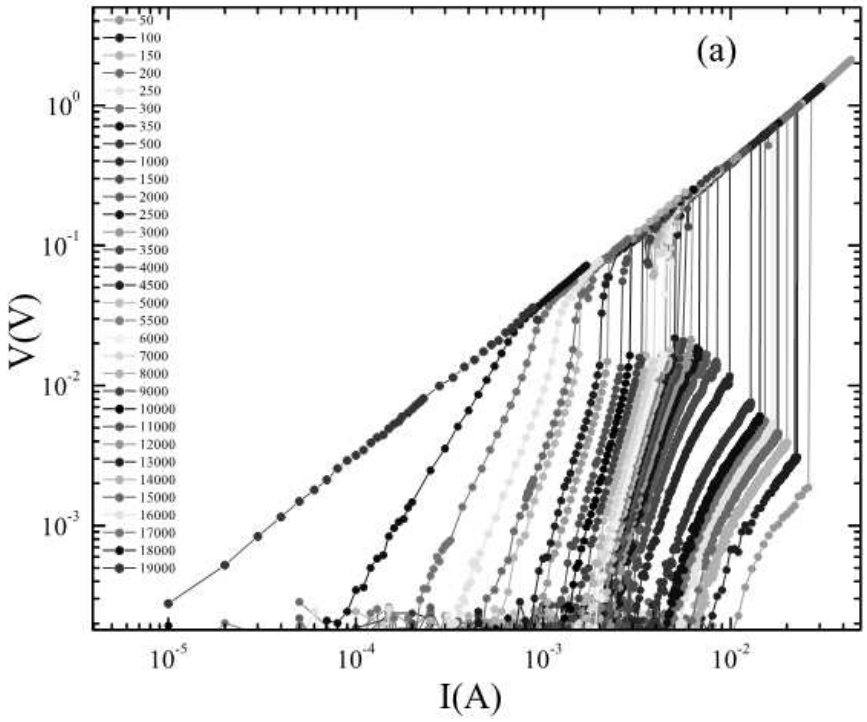

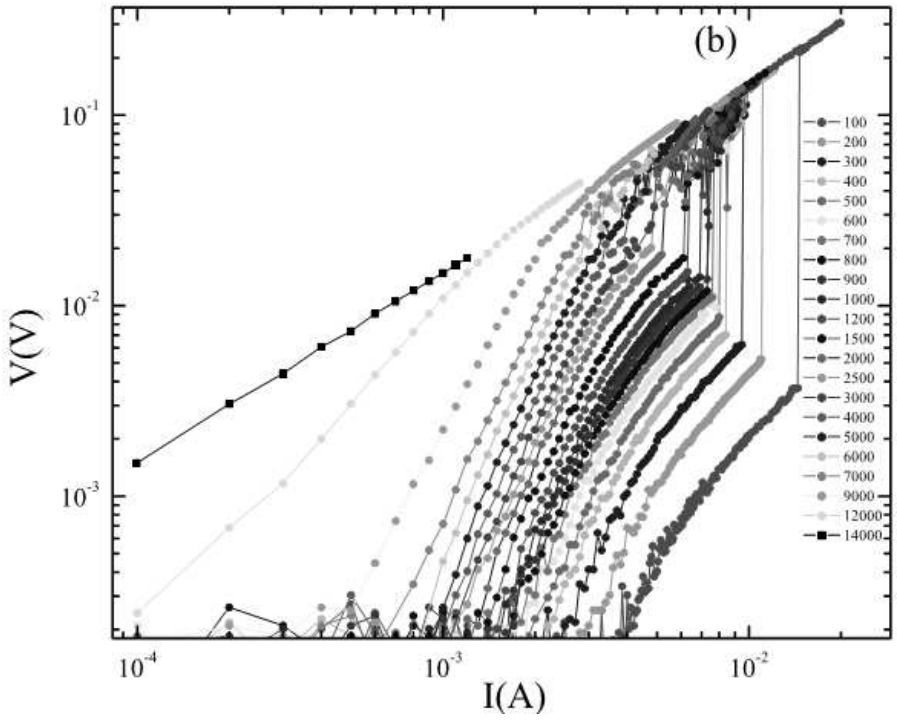

Figure 1.7: *I−V characteristics in double−logarithmic scale (a) for Nb (T = 4.2 K) and (b) Nb/PdNi (T =3.6 K) at various magnetic fields. Numbers in the figure indicate the values of the field in Oe. The reduced temperature is t ≈ 0.57 for both samples.*

The critical current density $J_c = I_c/wd$ (d is the sample thickness) at $t = 0.37$ for the two samples is shown in figure 1.8 as a function of the external magnetic field. The critical current I_c was defined using a dc electric field criterion of 10 mV cm^{-1}. J_c rises quickly when the field is lowered below H_{c2} and becomes more or less constant below $H_{c2}/2$. The values for J_c for the $Nb/Pd_{0.84}Ni_{0.16}$ bilayer are substantially lower than for the single Nb film and this is a consequence of the suppression of the superconducting order parameter inside the Nb layer due to the presence of the ferromagnet [11].

This result is very similar to that recently obtained on Nb/Py systems although in that case the suppression of the critical current was a bit larger due to the stronger ferromagnetic nature of Py [11].

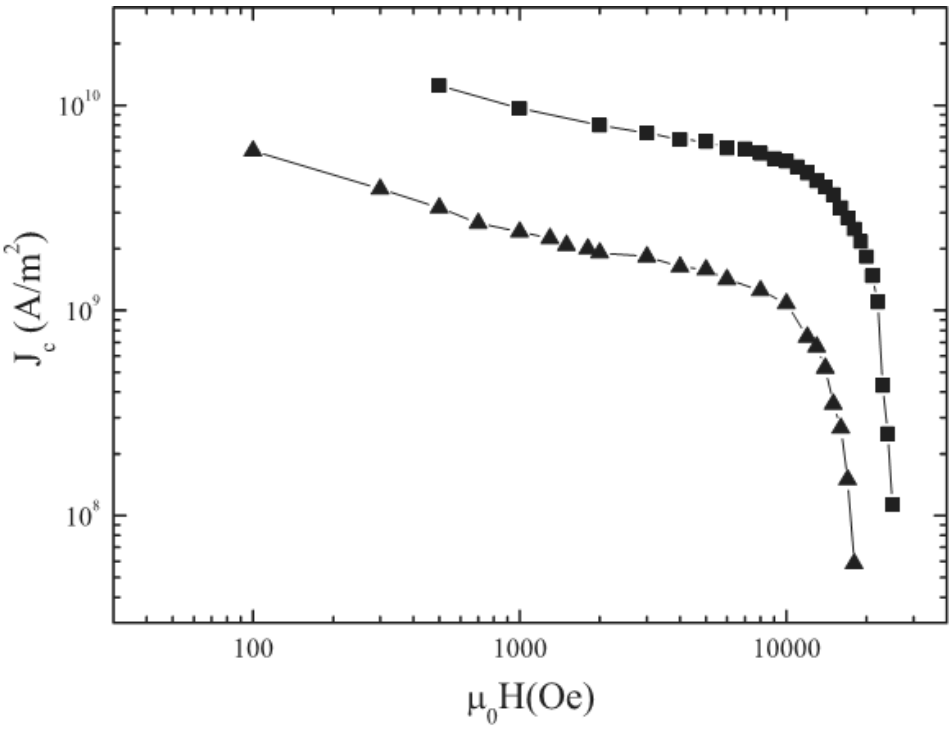

Figure 1.8: *Critical current density versus perpendicular magnetic field for the single Nb film (squares) at T = 2.7 K and for the Nb/PdNi bilayer (triangles) at T = 2.3 K. The reduced temperature is t ≈ 0.37 for both samples.*

1.4.2 Critical velocities

It is well known that, in the case of a vortex lattice which moves under high applied driving currents, a sudden jump from the flux flow to the normal state is present in the I−V curves at $I = I^*$ before reaching the value of the depairing critical current I_{dp} [33]. The voltage V^* at which the instability occurs can be expressed in terms of the so−called critical velocity v^* through the relation

$$V^* = \mu_0 v^* H L \tag{1.3}$$

where H is the applied magnetic field and L is the distance between the voltage contacts. The critical velocity is given by [33]

$$v^* = \frac{D^{1/2}[14\zeta(3)]^{1/4}(1-t)^{1/4}}{(\pi\tau_E)^{1/2}} \tag{1.4}$$

where D is the quasiparticle diffusion coefficient, $\zeta(3) = 1.202$ is the Riemann zeta function evaluated in 3 and τ_E is the inelastic scattering time of the quasiparticles. The specific temperature dependence of τ_E is related to the dominant relaxation mech-

anism: if electron−phonon interactions dominate it is $\tau_E \propto T^{-3}$, while if electron−electron interactions prevail it is $\tau_E = \tau_{E,el} \exp[2\Delta(T)/k_B T]$, where $\tau_{E,el}$ is the inelastic relaxation time of the electronic system and $\Delta(T)$ has the temperature dependence $\Delta(T) = \Delta(0)(1 - T/T_c)^{1/2}$, with $\Delta(0) \approx 1.76 k_B T_c$ as expected from BCS theory [11, 34, 35]. In figure 1.9 we show the values of v^* plotted as a function of H at $t = 0.43$ for the single Nb film and for the $Nb/Pd_{0.84}Ni_{0.16}$ bilayer.

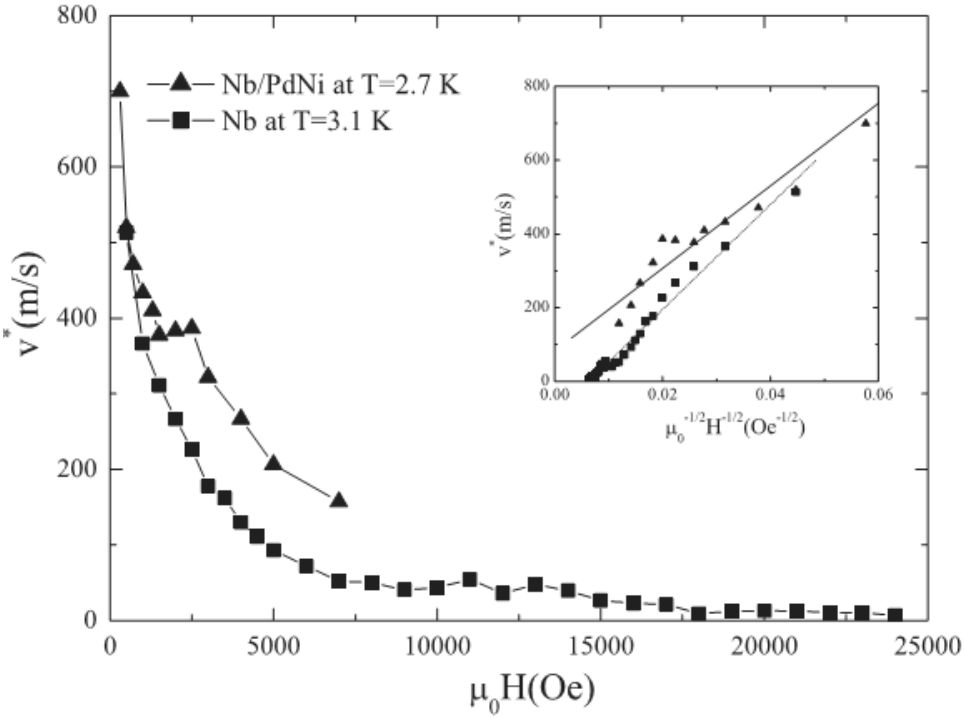

Figure 1.9: *Critical velocity v^* versus applied magnetic field at $t = 0.43$ for the 30 nm thick Nb film (squares) and for the Nb/Pd0.84Ni0.16 bilayer (triangles). Inset: v^* versus $H^{-1/2}$ at $t = 0.43$ for the Nb film (squares) and for the $Nb/Pd_{0.84}Ni_{0.16}$ bilayer (triangles). Lines are guides to the eyes to show the range in which the $H^{-1/2}$ proportionality of v^* is valid.*

The values for the critical velocity have been obtained from equation 2.1 assuming that the voltage V^* corresponds to the flux−flow instability of the vortex lattice. In the inset the behavior of v^* versus $H^{-1/2}$ at the same reduced temperature for both the samples is reported. In both cases the data show that the critical velocity is proportional to $H^{-1/2}$, indicating that thermal effects are not responsible for the observed instability [11, 34]. However, it has been noticed that the $H^{-1/2}$ dependence of the critical velocity can also be due to Joule heating [35–37]. In this case, if the dissipated power $P^* = I^* V^*$ at the voltage jumps is considered, a well−defined expression as a function of H/H_T is obtained where H_T is the magnetic field where thermal effects influence the flux−flow instabilities [11, 36–38]. In figure 1.10 the dissipated power P^* as a function of the magnetic field is reported for the $Nb/Pd_{0.84}Ni_{0.16}$ bilayer at one of the measured temperatures, namely $T = 3.26$ K.

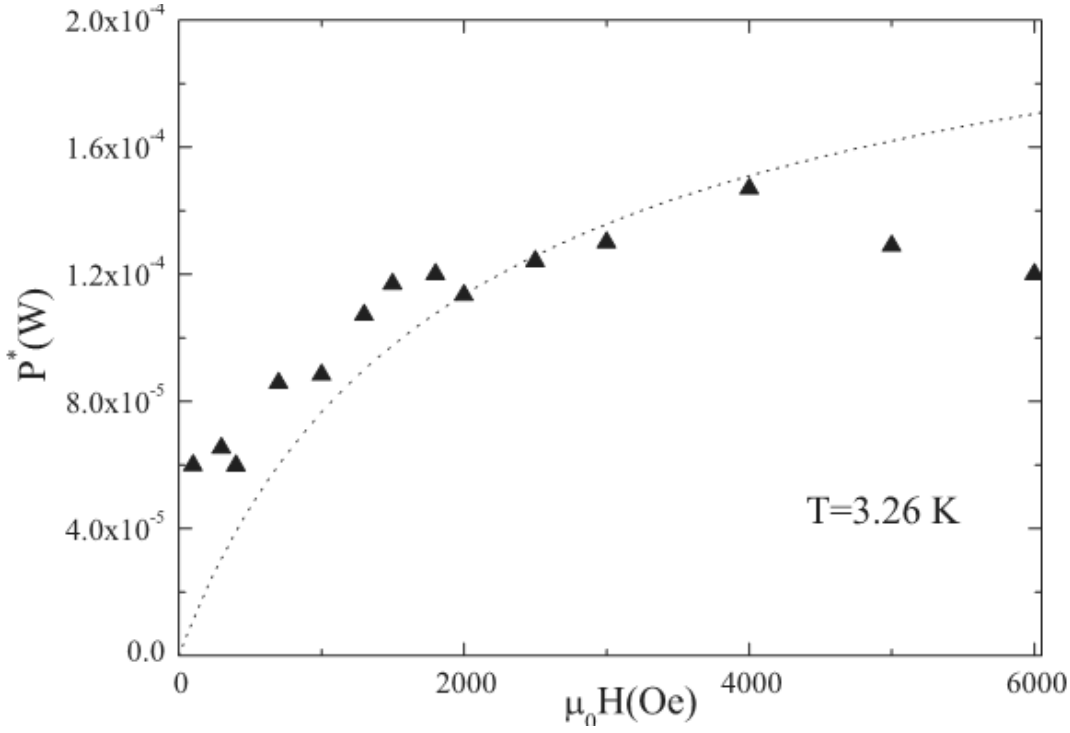

Figure 1.10: *Dissipated power at the onset of the voltage jumps as a function of the magnetic field at $T = 3.26$ K for the $Nb/Pd_{0.84}Ni_{0.16}$ bilayer. The dashed line is a fit to the experimental data using the Bezuglyj and Shklovskij theory [37].*

The dashed line is a fit to the experimental data using the theoretical expression [37] $P = P_0(1 - a)$, where $a = [1 + b + (b^2 + 8b + 4)^{1/2}]/[3(1 + 2b)]$ and $b = H/H_T$. We obtain $\mu_0 H_T = 0.3$ T but the agreement between experimental points and theory is rather unsatisfactory. For the $Nb/Pd_{0.84}Ni_{0.16}$ we get similar results at all the measured temperatures and no agreement with theory was found for the Nb film, implying that quasiparticle heating is not dominant in determining the magnetic field dependence of v^* [11, 37]. The results in figure 1.9 also show that the critical velocities in the case of the $Nb/Pd_{0.84}Ni_{0.16}$ bilayer are larger and, despite the comparable values of $H_{c2\perp}(t = 0.43)$ (for Nb $H_{c2\perp}(T = 3.1\text{K}) = 2.5$ T while for the $Nb/Pd_{0.84}Ni_{0.16}$ it is $H_{c2\perp}(T = 2.7\text{K}) = 2.3$ T), in the case of the $Nb/Pd_{0.84}Ni_{0.16}$ bilayer the instability already disappears at smaller fields without reaching a fairly constant value. As in the case of Nb/Py bilayers where, however, the critical velocity values were much larger [11] this result is due to the different values for the relaxation time τ_E for the two systems. The same data shown above for v^* are plotted in figure 1.11 as a function of H/H_{max} where with H_{max} we denote the highest field at which, at that reduced temperature ($t = 0.43$), the vortex instability is still present in the I−V curves for each of the two systems ($\mu_0 H_{max} = 2.4$ T for the single Nb film and $\mu_0 H_{max} = 0.7$ T for the $Nb/Pd_{0.84}Ni_{0.16}$ bilayer).

We see, for example, that at the reduced field $H/H_{max} = 0.4$ the values of the

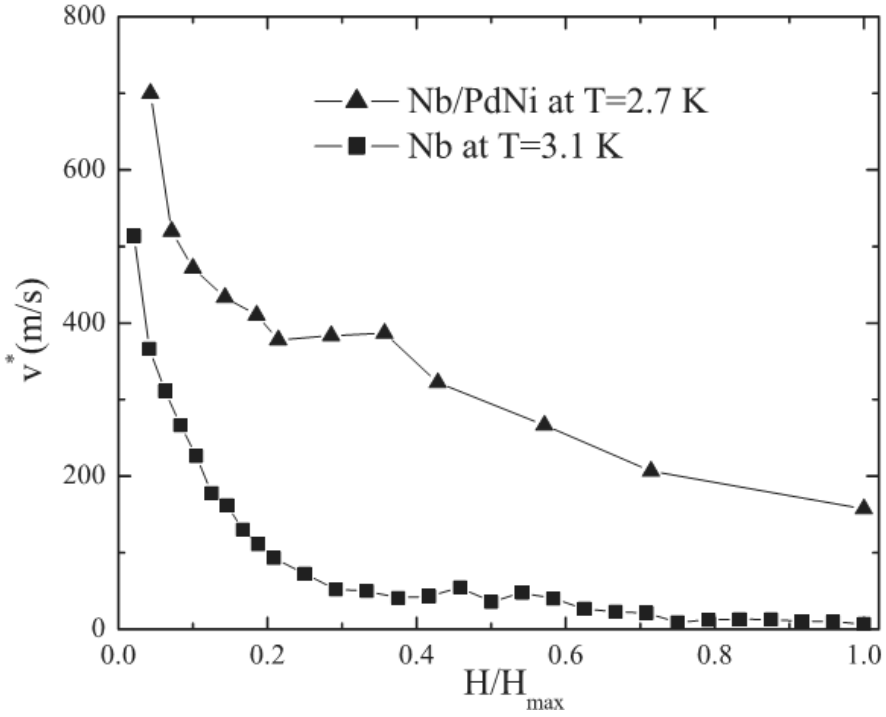

Figure 1.11: *v^* versus H/H_{max} at $t = 0.43$ for the 30 nm thick Nb film (squares) and for the $Nb/Pd_{0.84}Ni_{0.16}$ bilayer (triangles). H_{max} is the highest field where the vortex instability is present in the $I-V$ curves.*

critical velocities measured in the $Nb/Pd_{0.84}Ni_{0.16}$ bilayer are one order of magnitude higher which implies, from equation 2.1, that τ_E is two orders of magnitude smaller for this system ($\tau_E \propto 1/(v^*)^2$). In figure 2.3 the temperature dependence of τ_E is shown for the single Nb film at $\mu_0 H = 1.40$ T and $\mu_0 H = 0.90$ T, which correspond to $H/H_{max} = 0.56$ and $H/H_{max} = 0.37$, respectively. The solid and the dashed−dotted lines are fits of the experimental data to the equation $\tau_E = \tau_{E,el} exp[m\Delta(T)/k_B T]$ with $\tau_{E,el}$ and m both used as fitting parameters. We obtain $\tau_{E,el} = 2.0 \times 10^{-9}$ s and $m = 1.8$ at $\mu_0 H = 1.40$ T, and $\tau_{E,el} = 0.7 \times 10^{-9}$ sand $m = 1.75$ at $\mu_0 H = 0.90$ T.

This result shows that electron−electron scattering dominates the energy relaxation in Nb film and that the temperature dependence is mainly due to that of the gap [11]. Different is the case for the Nb/PdNi bilayer where, instead, τ_E shows a weak temperature dependence. Experimental data cannot be fitted with the exponential expression for τ_E unless we use a very small number for m ($m = 0.3$). The dashed and the dotted lines in figure 2.3 are fits of the experimental data to the power−law behavior $\tau_E \propto T^{-n}$ for the $Nb/Pd_{0.84}Ni_{0.16}$ sample at $\mu_0 H = 0.25$ T ($H/H_{max} = 0.36$, which is the same reduced field corresponding to $\mu_0 H = 0.90$ T for the single Nb film) and $\mu_0 H = 0.15$ T ($H/H_{max} = 0.21$). The values $n = 2.9$ and 2.6 are, respectively, obtained and this tells that, in contrast, in this sample the dominant relaxation mechanism may be electronphonon scattering [35]. This result is completely different with

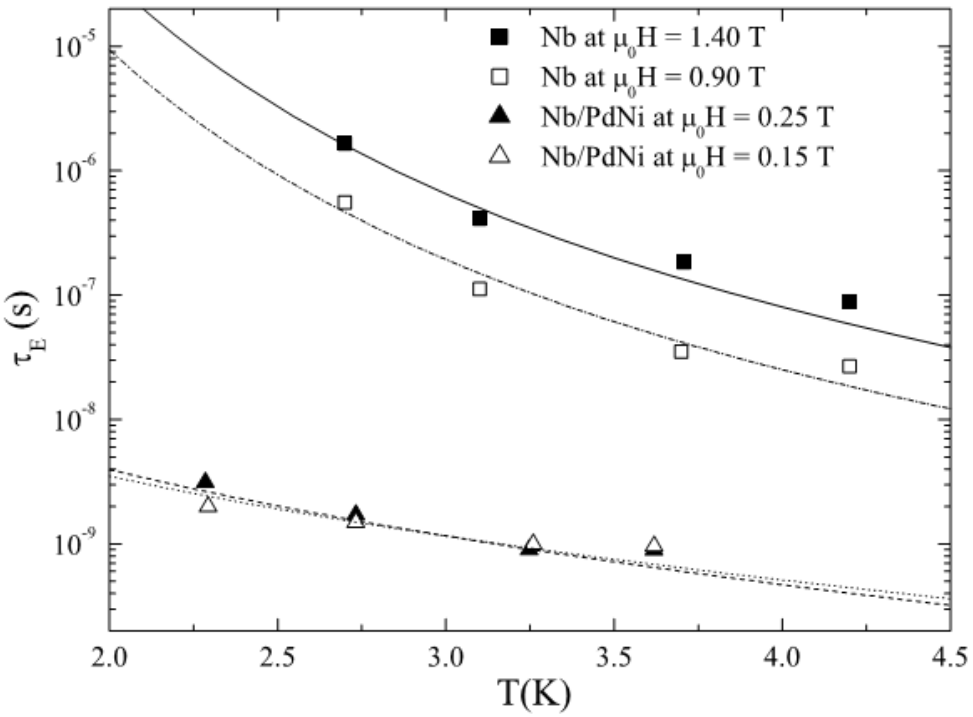

Figure 1.12: *τ_E temperature dependence for the Nb single film at $\mu_0 H$ =1.40 T (closed squares) and at $\mu_0 H$ = 0.90 T (open squares) and for Nb/Pd0.84Ni0.16 at $\mu_0 H$ = 0.25 T (closed triangles) and $\mu_0 H$ = 0.15 T (open triangles). The solid and the dasheddotted lines are the fits to the experimental data using the expression $\tau_E = \tau_{E,el}\ exp[m\Delta(T)/k_B T]$. The dashed and the dotted lines are the fits to the experimental data using the expression $\tau_E \propto T^{-n}$. See the text for details.*

respect to what was obtained for the Nb/Py system [11]. In that case the relaxation mechanism was still electronelectron scattering but the coefficient m was equal to 1.0 because the effective gap experienced by the quasiparticles in their relaxation process was almost half of the Nb gap. Therefore the larger critical velocities for vortices in the Nb/Py were directly connected to the suppression of the superconducting order parameter in the S layer. In the case of $Nb/Pd_{0.84}Ni_{0.16}$, due to the weaker ferromagnetic nature of the alloy, the order parameter is less suppressed in the superconductor and this implies, as we have observed, higher critical currents and smaller critical velocities with respect to Nb/Py. However, due to the larger value of ξ_{PdNi} with respect to ξ_{Py}, the superconductivity in the case of $Nb/Pd_{0.84}Ni_{0.16}$ penetrates on longer distances in the ferromagnet with respect to the Nb/Py where it was essentially confined only in the Nb layer. This could be responsible of the different relaxation mechanism observed for the $Nb/Pd_{0.84}Ni_{0.16}$ system.

1.5 Conclusions

We have studied the I−V characteristics at different perpendicular magnetic fields and temperatures for an Nb/$Pd_{0.84}Ni_{0.16}$ bilayer. Critical currents are smaller than those measured in the single Nb film with the same thickness. Sudden jumps in the I−V curves due to the instability of the moving vortex lattice have also been observed and the values of the critical velocities connected to the measured instabilities are larger in Nb/$Pd_{0.84}Ni_{0.16}$ with respect to the single Nb. The above experimental findings were consistently interpreted as due to the depression of the superconducting order parameter in the Nb layer when in contact with the weak ferromagnet. Moreover, the penetration of superconductivity in the F layer over distances of a few nanometers could be responsible for the change of relaxation mechanism observed in Nb/$Pd_{0.84}Ni_{0.16}$ with respect to the one which was obtained for the single Nb film.

Bibliography

[1] A. I. Buzdin, Rev. Mod. Phys. **77**, 935 (2005).

[2] J. S. Jiang ,D. Davidovic ,D. H. Reich and C. L. Chien, Phys. Rev. Lett. **74**, 314 (1995).

[3] Th. M*ü*hge, N. N. Garifyanov, Y. V. Goryunov, G. G. Khaliullin, L. R. Tagirov, K. Westerholt, I. A. Garifullin and H. Zabel, Phys. Rev. Lett. **77** 1857, (1996).

[4] Y. Obi, M. Ikebe and H. Fujishiro, Phys. Rev. Lett. **94** 057008 (2005).

[5] V. A. Oboznov, V. V. Bolginov, A. K. Feofanov, V. V. Ryazanov and A. I. Buzdin Phys. Rev. Lett. **96** 197003 (2006).

[6] E. A. Demler, G. B. Arnold and M. R.Beasley, Phys. Rev. B **55** 15174 (1997).

[7] Y. V. Fominov, N. M. Chtchelkatchev and A. A. Golubov, Phys. Rev. B **66** 014507(2002).

[8] C. Cirillo, C. Bell, G. Iannone, S. L. Prischepa, J. Aarts and C. Attanasio, Phys. Rev. B **80** 094510(2009).

[9] J. M. E. Geers, M. B. S. Hesselberth, J. Aarts and A. A. Golubov Phys. Rev. B **64** 094506 (2001).

[10] C. Cirillo, A. Rusanov, C. Bell and J. Aarts, Phys. Rev. B **75** 174510 (2007).

[11] A. A. Armenio, C. Bell, J. Aarts and C. Attanasio, Phys. Rev. B 76 054502 (2007).

[12] J. Guimpel, M. E. de la Cruz, F. de la Cruz, H. J. Fink, O. Laborde and J. C. Villegier, J. Low Temp. Phys. **63** 151 (1986).

[13] Z. Radovic, L. Dobrosavljevic-Grujic, A. I. Buzdin and J. R. Clem, Phys. Rev. B **38** 2388 (1988).

[14] P. Koorevaar, Y. Suzuki, R. Coehoorn and J. Aarts, Phys. Rev. B **49** 441 (1994).

[15] C. Cirillo, S. L. Prischepa, M. Salvato, C. Attanasio, M. Hesselberth and J. Aarts, Phys. Rev. B **72** 144511 (2005).

[16] A. Bauer, J. Bentner, M. Aprili, M. L. Della Rocca, M. Reinwald, W. Wegscheider and C. Strunk, Phys. Rev. Lett. **92** 217001 (2004).

[17] K. Matsuda, Y. Akimoto, T. Uemura and M. Yamamoto J. Appl. Phys. 103 07C711 (2008).

[18] T. S. Khaire, W. P. Jr. Pratt and N. O. Birge Phys. Rev. B **79** 094523 (2009).

[19] E. H. Sondheimer, Phys. Rev. **80** 401 (1950).

[20] A. Potenza and C. H. Marrows Phys. Rev. B **71** 180503(R) (2005).

[21] A. A. Armenio, C. Cirillo, G. Iannone, S. L. Prischepa and C. Attanasio Phys. Rev. B **76** 024515 (2007).

[22] J. Aarts, J. M. E. Geers, E. Brück, A. A. Golubov and R. Coehoorn, Phys. Rev. B **56** 2779 (1997).

[23] L. Dumoulin, P. Nedellec and P. M. Chaikin, Phys. Rev. Lett. **47** 208 (1981).

[24] J. Kim, J. H. Kwon, K. Char, H. Doh and H-Y. Choi Phys. Rev. B **75** 014518 (2005).

[25] A. S, Sidorenko, V. I. Zdravkov, A. A. Prepelitsa, C. Helbig, Y. Luo, S. Gsell, M.Schreck, S. Klimm, S. Horn, L. R. Tagirov and R . Tidecks Ann. Phys., Lpz. **12** 37 (2003).

[26] T. Kontos, M. Aprili,J. Lesueur and X. Grison, Phys. Rev. Lett. **86** 304 (2001).

[27] T. Kontos, M. Aprili,J. Lesueur, F. Genet, B. Stephanidis and R. Boursier, Phys. Rev. Lett. **89** 137007 (2002).

[28] T. Kontos, M. Aprili, J. Lesueur, X. Grison and L. Dumoulin, Phys. Rev. Lett. **93** 137001 (2004).

[29] A. Y. Rusanov, J. Aarts and M. Aprili 2006 Proc. NATO Advanced Research Workshop on Nanoscale DevicesFundamentals and Applications (Kishinev, Moldova, 1822 Sept. 2004): NATO Science Series II: Mathematics, Physics and Chemistry vol 233 ed R Gross, A. Sidorenko and L. Tagirov (New York: Springer) p 127.

[30] M. L. Della Rocca, PhD Thesis Università degli Studi di Salerno (2003).

[31] T. Kontos, PhD Thesis Université Paris XI Orsay (2002).

[32] J. Aarts, C. Attanasio, C. Bell, C. Cirillo, M. Flokstra and J. M. Knaap v d Nanoscience and Engineering in Superconductivity ed V Moshchalkov, R Woerdenweber and W Lang (New York: Springer) p 323 (2010).

[33] A. I. Larkin and Y. N. Ovchinnikov Sov. Phys.JETP **41** 960 (1976).

[34] S. G. Dottinger, S. Kittelberger, R. P. Huebener and C. C. Tsuei, Phys. Rev. B **56** 14157 (1997).

[35] B. J. Ruck, H. J. Trodhal, J. C. Abele and M. J. Geselbracht, Phys. Rev. B **62** 12468 (2000).

[36] C. Peroz and C. Villard, Phys. Rev. B **72** 014515 (2005).

[37] A. I. Bezuglyj and V. A. Shklovskij Physica C **202** 234 (1992).

[38] Z .L. Xiao, P. Voss-de Haan, G. Jakob and H. Adrian Phys. Rev. B **57** R736 (1998).

Chapter 2

Quasiparticles relaxation processes in Nb/CuNi bilayers

The dynamic instability of the moving vortex lattice at high driving currents has been studied in superconductor (S)/weak ferromagnet (F) bilayer, $Nb/Cu_{0.38}Ni_{0.62}$. Voltage-current, V (I), characteristics have been acquired as a function of both the temperature, T, and the magnetic field, H, and interpreted in the framework of the model proposed by Larkin and Ovchinnikov. From these analysis the values of the quasiparticle relaxation time, τ_E, have been estimated. The results confirm the high performance of S/F hybrids in terms of velocity in the energy relaxation process, compared to corresponding single superconducting thin films. Moreover the temperature dependence of τ_E is extremely smooth, also if compared with the data reported in literature for other weak ferromagnet S/F based systems. This last result has been tentatively ascribed to the disorder present in the CuNi alloy.

2.1 Introduction

The investigation of the interplay between superconductivity and ferromagnetism always provides new insights. Starting from an intensive fundamental research in this field [1, 2], many suggestions have afterwards been proposed for applications [3, 4]. Recently the attention focused also on vortex lattice instability [5–7] and on non-equilibrium superconductivity [8–10], both subjects being important in the design of S/F-based devices, such as, for instance, optical detectors.

This Chapter is devoted to the study of the dynamic of the vortex lattice in Nb/CuNi bilayer in order to estimate both the values and the temperature dependence of the inelastic scattering time of the quasiparticles, τ_E [11]. The main purpose is to deepen the knowledge of the relaxation mechanisms present in S/F hybrids, which seem to be deeply affected by the presence and the nature of the ferromagnetic layer. The approach is based on the model proposed by Larkin and Ovchinnikov (LO) [12]. The latter, already applied in the case of different superconducting systems [13–15] and S/F bilayers [5–7], consists in the analysis of the V (I) characteristics at different temperatures, T, and magnetic fields, H. At high driving currents in fact, due to the presence of the electric field inside the vortex core, the quasiparticles escape from these normal regions and relax their energy inside the condensate, with a characteristic relaxation rate [13]. This process causes a continuous shrinkage of the vortex core until a critical velocity, v^*, is reached, such that the system switches into the normal state. From the theory of LO, v^* is directly related to the relaxation time, according to

$$v^* = \frac{D^{1/2}[14\zeta(3)]^{1/4}(1-t)^{1/4}}{(\pi\tau_E)^{1/2}} \tag{2.1}$$

where D is the quasiparticle diffusion coefficient, $\zeta(3) = 1.202$ is the Riemann zeta function evaluated in 3, and $t = T/T_c$ is the reduced transition temperature. Moreover, the temperature dependence of τ_E reveals the dominant relaxation process in the system: (a) $\tau_E = \tau_{e-e} exp(2\Delta(T)/k_B T)$ electron-electron recombination [11]; (b) $\tau_E \propto T^{-3}$, electron-phonon scattering [12]. Recently it has been shown that the presence of the ferromagnet in S/F bilayers strongly increases the values of the critical velocity at which the instability sets in, thus shortening the relaxation processes, according to 2.1. This result has been confirmed for hybrids consisting on both Nb [5, 6] and NbN [7] superconducting layer. In the case of Nb-based hybrids the study has been performed employing F layers characterized by different exchange energy, such as strong Py [5], as well as weak PdNi [6] ferromagnets. What is worth to mention is the clear difference in the temperature dependence of the relaxation time in these two systems. τ_E presents in fact a much weaker temperature dependence in the case of the Nb/PdNi bilayer, which could be a signature of a dominant electron-phonon scattering. Both the low values of τ_E and the weak temperature dependence are features which could be desirable in the design of optical detection devices. For this reason the main scope of this Chapter is perform an analogous analysis of the critical velocity measurements at different values of the applied magnetic field for a system consisting of Nb as superconducting layer and another weak ferromagnet as F layer, namely Nb/CuNi.

2.2 Samples fabrication and preliminary characterization

The Nb/CuNi bilayer has been grown on Si(100) substrates by a UHV dc diode magnetron sputtering operating at a base pressure of 2×10^{-8} mbar. The deposition has been performed at room temperature at an Ar pressure of 1×10^{-3} mbar. The typical deposition rates were 0.28 nm s^{-1} for Nb and 0.21 nm s−1 for CuNi, measured by a quartz crystal monitor previously calibrated by low-angle X−ray reflectivity measurements on deliberately deposited thin films of each material. The Ni concentration in the CuNi films, estimated by energy dispersion spectrometry analysis (EDS), is $x = 0.62$. According to literature, this Ni content should correspond to an exchange energy $E_{ex} \approx 13$ meV [17, 18]. The sample consists of a Nb and a CuNi layer with thicknesses $d_{Nb} = 30$ nm and $d_{CuNi} = 80$ nm, respectively. The ferromagnetic thickness has been chosen to be well above the CuNi coherence length, $\xi_F \propto 1/\sqrt{E_{ex}} \approx$ 3−6 nm [17–19]. For comparison a reference Nb film, 30 nm thick, has been also sputtered in the same deposition run of the bilayer. Standard optical lift-off technique has been employed to pattern the samples in a bridge geometry with width w=20 μm and length L =300 μm. The superconducting critical temperature of the single Nb film and of the Nb/CuNi bilayer, in absence of any applied magnetic field, are $T_c^{Nb} =$ 7.3 K and $T_c^{CuNi} = 6.5$ K, respectively. The voltage-current characteristics have been acquired using the standard dc four probe technique, biasing the samples with current pulses, $t_{pulse} = 12$ ms, in order to avoid heating effects. The detailed description of the measurement procedure as well as the analysis of the dissipated power are extensively reported in references [5–7]. V (I) characteristics have been measured in presence of a magnetic field applied perpendicularly to both the plane of the substrate and the direction of the current.

2.3 Current-voltage characteristics

The voltage-current characteristics for both the systems have been preliminary measured at zero applied magnetic field. In this way it was possible to estimate the values of the critical current densities as $J_c = I_c/wd$ (here $d = d_{Nb} + d_{CuNi}$), assuming a voltage criterion of 10 mV/cm. At the reduced temperature, $t = T/T_c \approx 0.6$, the values of the critical current density are $J_c^{Nb/CuNi}$ =2.5×10^9 A/m^2 and J_c^{Nb} =4.3 × 10^{10} A/m^2. The depression of J_c for the Nb/CuNi bilayer can be ascribed to the suppression of the superconducting order parameter inside the Nb layer due to the

presence of the ferromagnet, as it has been already reported for other S/F systems, based on both strong [5] and weak ferromagnets [6]. V (I) characteristics have been measured for the Nb/CuNi bilayer as a function of the magnetic field at different temperatures, namely $T = 3.60$, 3.23, 2.67, 2.32 K ($t = 0.55$, 0.50, 0.41, 0.36). In the case of the reference Nb bridge the V (I) curves have been acquired only at $T = 4.2$ K($t = 0.57$). The V (I) characteristics of the Nb/CuNi structure at $T = 3.60$ K are shown in Figure 2.1.

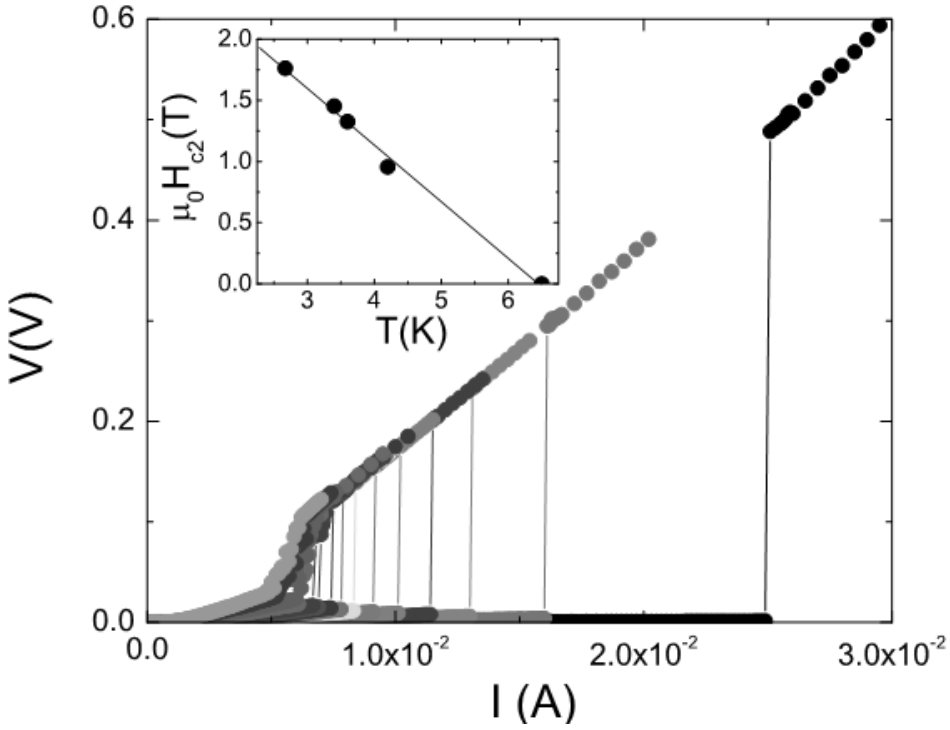

Figure 2.1: *V (I) characteristics as a function of the magnetic field measured at $T = 3.6$ K for the Nb/CuNi bilayer. The values of the magnetic field are from right to left, 0, 0.01, 0.02, 0.03, 0.04, 0.05, 0.06, 0.07, 0.08, 0.09, 0.10, 0.12, 0.15, 0.20, 0.25 T. Inset: temperature dependence of the perpendicular upper critical magnetic field for the Nb/CuNi bilayer.*

From the data it is evident that, at small applied magnetic field, the transitions to the normal state are quite abrupt, until the voltage jumps disappear at $\mu_0 H \approx 0.1$ T. As already discussed in the introduction, this result has been interpreted in the framework of the model proposed by Larkin and Ovchinnikov [12]. According to the theory the voltage jumps, V^*, are related to the critical vortex velocity, v^*: $V^* = \mu_0 v^* HL$. In this way, from the analysis of the V (I) curves, it is possible to evaluate the behavior of the critical velocity as a function of both the temperature and the magnetic field. In Figure 2.2 the dependence of v^* as a function of the reduced field, H/H_{max}, is reported for both the single Nb bridge and the Nb/CuNi bilayer at the reduced temperature $t = T/T_c = 0.57$ and $t = 0.55$, respectively, where H_{max}, once the temperature is fixed, is the maximum field at which the voltage jump is still present.

Here $\mu_0 H_{max} = 1$ T for Nb single film and $\mu_0 H_{max} = 0.1$ T for the Nb/CuNi bilayer.

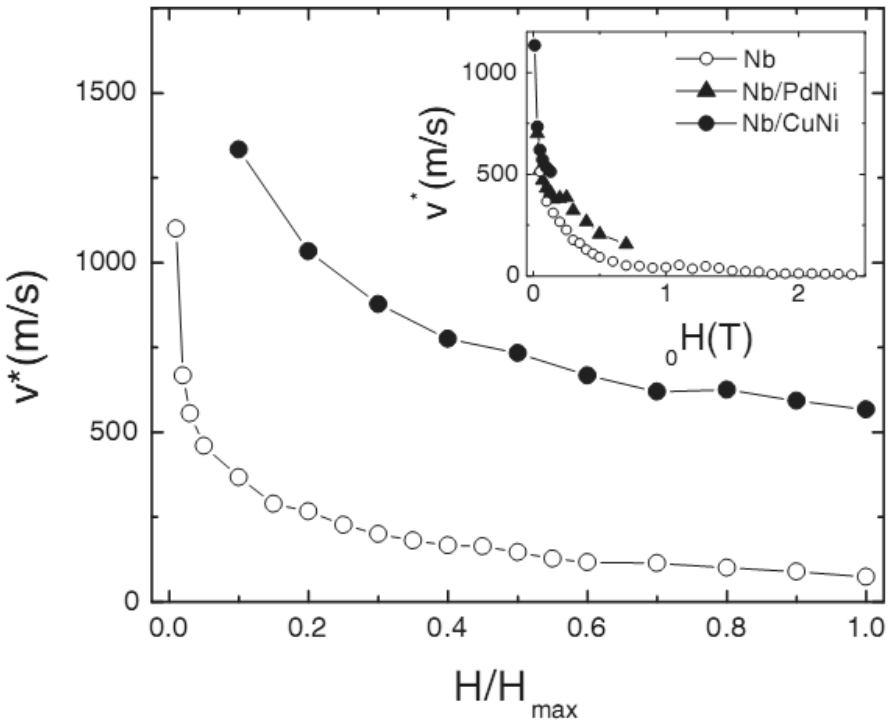

Figure 2.2: *Dependence of the critical velocity, v^*, on the normalized magnetic field H/H_{max} for the Nb single film at $t = 0.57$ (open symbols) and the Nb/CuNi bilayer at $t = 0.55$ (closed symbols). For the definition of H_{max} the reader can refer to the text. Inset: dependence of v^* on the magnetic field H at $t = T/T_c \approx 0.4$ for the Nb single film (open symbols), and the Nb/CuNi (closed circles) and the Nb/PdNi (closed triangles) bilayers [6].*

It is evident that, in agreement with the data reported in literature [5–7], the S/F bilayer presents higher critical velocities, which, moreover, disappear at a much lower value of the magnetic field. This feature is strongly pronounced for the Nb/CuNi system as highlighted in the inset of Figure 2.2, where the field dependence of v^* is compared to one obtained for the Nb/PdNi bilayer [6]. Here the $v^*(H)$ dependence is reported for the single Nb film, and both the Nb/CuNi and the Nb/PdNi bilayers at $t = T/T_c \approx 0.4$. At this reduced temperature the value of H_{max} for the Nb/PdNi system is in fact 0.7 T. At this point, according to 2.1, τ_E can also be calculated. The quasiparticle diffusion coefficient has been estimated from the slope of the temperature dependence of the perpendicular upper critical magnetic field, $H_{c2}(T)$, as $D = (4k_B/\pi e) \times (dH_{c2}/dT|_{T=T_c})^{-1}$. The $H_{c2}(T)$ curve has been in fact resistively obtained from the $R(H)$ transitions measured at constant temperature. The $H_{c2}(T)$ dependence is presented in the inset of Figure 2.2, where the line is the linear fit with slope $(dH_{c2}/dT|_{T=Tc}) = -0.46$ T/K. It follows that $D = 2.0 \times 10^{-4} m^2/\text{s}$. The temperature dependence of the relaxation time for the Nb/CuNi bilayer for different values of the magnetic fields is reported in Figure 2.3.

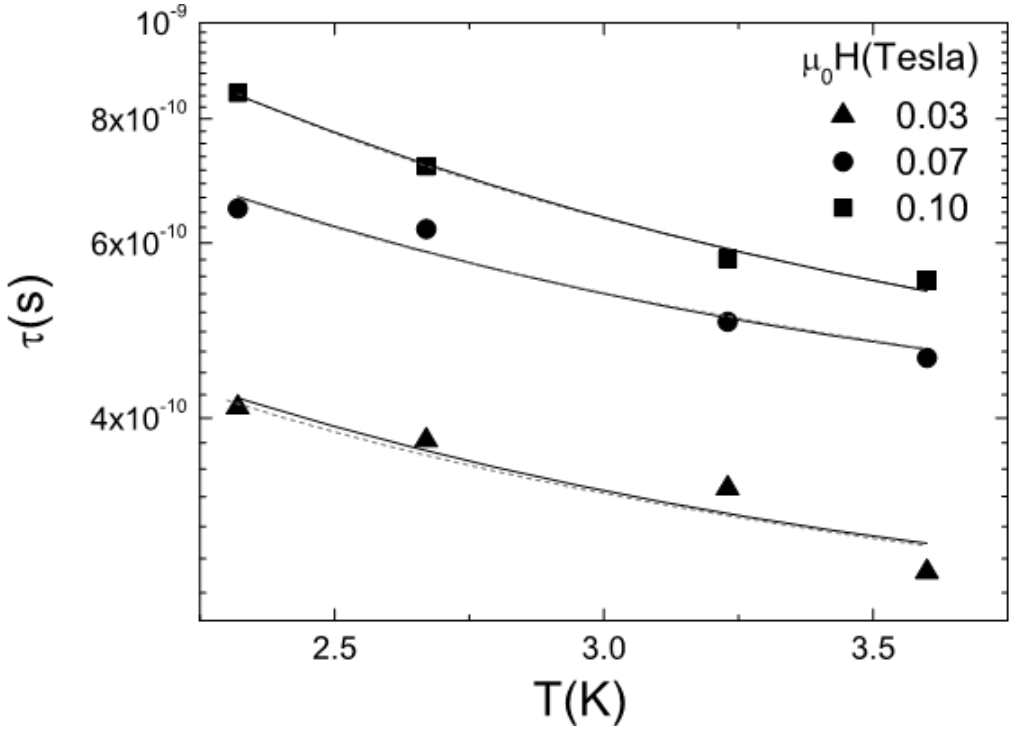

Figure 2.3: *Temperature dependence of the relaxation time, τ_E, for the Nb/CuNi bilayer at $\mu_0 H$ = 0.10 T (squares), 0.07 T (cirles) and 0.03 T (triangles). The dashed lines are the fits to the experimental data using the expression $\tau_E = \tau_{e-e}\ exp(2\Delta(T)/k_B T)$. The solid lines are the fits to the experimental data using the expression $\tau_E \propto T^{-n}$. The reader can refer to the text for further details.*

In order to extract information regarding the inelastic relaxation process responsible of this behavior, the experimental data have been fitted using the exponential and the power law dependencies described in the introduction. The dashed lines in Figure 2.3 are the best fit of the data using the expression $\tau_E = \tau_{e-e} exp(2m\Delta(T)/k_B T)$ with τ_{e-e} and m both used as fitting parameters. The agreement with the experiment is satisfactory only using a very small value for m, namely m =0.18−0.25. The solid lines reproduce the power law behavior $\tau_E \propto \mathrm{T}^{-n}$ where n =0.95, 0.72, 0.68 at $\mu_0 H$ = 0.10, 0.07, 0.03 T, respectively. All the fitting parameters are summarized in Table 2.1. The value obtained for the fitting parameter m from the exponential law dependence seems to exclude the electron-electron recombination as the dominant relaxation process in the system, since the small exchange energy of the ferromagnetic alloy would not suppress the superconducting gap so drastically.

The same result has been obtained also for other two S/F hybrids consisting of a weak ferromagnet, namely Nb/PdNi (m = 0.3 both at $\mu_0 H$ = 0.25 and 0.15 T) [6] and NbN/CuNi (m = 0.5 at $\mu_0 H$ = 0.10 T) [7], in contrast with what reported for Nb/Py bilayers (m = 1.0 at $\mu_0 H$ = 0.15 T) [5]. However, the power law simulations also return an extremely low value of $n \approx 0.7$−1.0, thus preventing the confirmation

$\mu_0 H$	τ_{e-e} (s)	m	n
0.10	3.17×10^{-10}	0.25	0.95
0.07	3.12×10^{-10}	0.19	0.72
0.03	2.03×10^{-10}	0.18	0.68

Table 2.1: *Summary of the fitting parameters extracted from the analysis of the $\tau_E(T)$ dependence for the Nb/CuNi bilayer.*

of a dominant electron-phonon scattering mechanism, in contrast with what reported for Nb/PdNi (n =2.6, 2.9 at $\mu_0 H = 0.25$ and 0.15 T, respectively) [6] and NbN/CuNi ($n = 2.0$ at $\mu_0 H = 0.10$ T) [7] bilayers. For these systems it was supposed that the weak ferromagnetic nature of the alloys caused a longer penetration in the F layer of the Cooper pairs, which could then experience different relaxation mechanism. Here the strength of the ferromagnet is comparable, but indeed the decay of the relaxation rate is much smoother. It seems reasonable to suppose that the reason of this dependence is the disorder of the CuNi alloy [20–23]. The latter, in fact, could make the bilayer as a whole a dirtier system. This would produce, not only a quasi-constant $\tau_E(T)$ dependence, but also an appreciable reduction of the quasiparticles lifetime [24]. Regarding this last point it is worth to comment on the comparison between the values of the relaxation time estimated for the Nb/CuNi bilayer and for the Nb bridge. The latter, at $t = 0.6$ and at $\mu_0 H = 1$ T ($H/H_{max} = 1$), for$(dH_{c2}/dT|_{T=T_c})= -0.62$ T/K, and consequently, $D = 1.7 \times 10^{-4}$ m^2/s, is characterized by a scattering rate $\tau_E^{Nb} = 2.7 \times 10^{-8}$ s. This value is consistent with the ones estimated with the same approach for single Nb films [5, 6], but it is two orders of magnitude higher than the one estimated for the corresponding Nb/CuNi bilayer at the same values of reduced temperature and magnetic field, namely $\tau_E^{Nb/CuNi} \approx 5.5 \times 10^{-10}$ s. Moreover, compared Nb/PdNi bilayers at the same value of $t \approx 0.5$ and $H/H_{max} \approx 0.3$, the response of the Nb/CuNi device appears to be the faster, since $\tau_E^{Nb/PdNi} \approx 9{\times}10^{-10}$ s [6], while $\tau_E^{Nb/CuNi} \approx 3{\times}10^{-10}$ s. This last result supports the hypothesis that the cleaness of the samples plays a crucial role in the relaxation process [24]. One last comment could be made if one compares the numbers reported in this work with the ones estimated for NbN/CuNi bilayers, namely a system constituted of the same disordered ferromagnetic alloy. In that case the quasiparticle lifetime was significantly shorter, also due extremely reduced characteristic e-ph scattering times of NbN thin films [25]. At $t \approx 0.5$ and $H/H_{max} \approx 0.5$ it was obtained $\tau_E^{NbN/CuNi} \approx 3 \times 10^{-11}$ s [7]. However the decay of the relaxation rate was faster that the one estimated in this work. It seems fair to suppose that this was due to the presence of an ultrathin CuNi overlayer, being $d_{CuNi} < \xi_F$. On the contrary here the ferromagnetic thickness exceeded ξ_F by far, and consequently the quasiparticles can penetrate the F layer over the entire ferromagnetic coherence length, experiencing different microscopic relaxation mechanisms.

2.4 Conclusions

V (I) characteristics have been measured on Nb/CuNi bilayers and interpreted in the framework of the LO theory [12]. In this way the values of the quasiparticles relaxation times have been estimated and compared to the ones obtained for the Nb reference sample. τ_E for the Nb/CuNi structure is about two orders of magnitude shorter compared to the values extracted for the corresponding Nb bridge. Moreover the τ_E shows an extremely smooth temperature dependence. Both the values of τ_E and its temperature dependence have been compared to the one observed in the case of other S/F bilayers consisting of weak ferromagnets [6, 7]. From this analysis it was concluded that the extremely disordered nature of the ferromagnetic alloy plays a crucial role in the relaxation processes.

Bibliography

[1] A. I. Buzdin, Rev. Mod. Phys. **77**, 935 (2005).

[2] F.S. Bergeret, A.F. Volkov, K.B. Efetov, Rev. Mod. Phys. **77**, 1321 (2005).

[3] A.K. Feofanov, V.A. Oboznov, V.V. Bolginov, J. Lisenfeld, S. Poletto, V.V. Ryazanov, A.N. Rossolenko, M. Khabipov, D. Balashov, A.B. Zorin, P.N. Dmitriev, V.P. Koshelets, A.V. Ustinov, Nature Phys. **6**, 593 (2010).

[4] I.P. Nevirkovets, M.A. Belogolovskii, Supercond. Sci. Technol.**24** , 024009 (2011).

[5] A.A. Armenio, C. Bell, J. Aarts, C. Attanasio, Phys. Rev. B **76**, 054502 (2007).

[6] C.Cirillo, E.A. Ilyina, C. Attanasio, Supercond. Sci. Technol. **24**, 024017 (2011).

[7] C. Cirillo, V. Pagliarulo, H. Myoren, C. Bonavolont‘ a, L. Parlato, G.P. Pepe, C. Attanasio, Phys. Rev. B **84**, 054536 (2011).

[8] N. Marrocco, G.P. Pepe, A. Capretti, L. Parlato, V. Pagliarulo, G. Peluso, A. Barone, R. Cristiano, M. Ejrnaes, A. Casaburi, N. Kashiwazaki, T. Taino, H. Myoren, R. Sobolewski, Appl. Phys. Lett. **97**, 092504 (2010).

[9] D. Pan, G.P. Pepe, V. Pagliarulo, C. De Lisio, L. Parlato, M. Khafizov, I. Komissarov, R. Sobolewski, Phys. Rev.B, **78**, 174503 (2008).

[10] T. Taneda, G.P. Pepe, L. Parlato, A.A. Golubov, R. Sobolewski, Phys. Rev. B **75**, 174507 (2007).

[11] S.B. Kaplan, C.C. Chi, D.N. Langenberg, J.J. Chang, S. Jafarey, D. Scalapino, Phys. Rev. B **14**, 4854 (1976), and references therein.

[12] A.I. Larkin, Yu.N. Ovchinnikov, Zh. Eksp. Teor. Fiz. **68**, 1915 (1975) [Sov. Phys. JETP , 960 (1976)].

[13] W. Klein, R.P. Huebener, S. Gauss, J. Parisi, J. Low Temp. Phys. **61** , 413 (1985).

[14] S.G. Doettinger, S. Kittelberger, R.P. Huebener, C.C. Tsuei, Phys. Rev. B **56**, 14157 (1997).

[15] Z.L. Xiao, P. Voss-de Haan, G. Jakob, Th. Kluge, P. Haibach, H. Adrian, E.Y. Andrei, Phys. Rev. B **59**, 1481 (1999).

[16] A.I. Larkin, Yu.N. Ovchinnikov, Zh. Eksp. Teor. Fiz. **73**, 299 (1977) [Sov. Phys. JETP **46**, 155 (1977)].

[17] J. Kim, J.H. Kwon, K. Char, H. Doh, H.-Y.Choi,Phys. Rev. B **72**, 014518 (2005).

[18] A.Yu. Rusanov, Ph.D. thesis, Leiden University (2005).

[19] C. Cirillo, C. Bell, G. Iannone, S.L. Prischepa, J. Aarts, C. Attanasio, Phys. Rev. B **80**, 094510 (2009).

[20] B. Mozer, D.T. Keating, S.C. Moss, Phys. Rev. **175**, 868 (1968).

[21] T.S. Khaire, W.P. Pratt Jr., N.O. Birge, Phys. Rev. B **79**, 094523 (2009).

[22] G. Iannone, D. Zola, A.A. Armenio, M. Polichetti, C. Attanasio,Phys.Rev.B **75**, (2007).

[23] V.N. Kushnir, S.L. Prischepa, J. Aarts, C. Bell, C. Cirillo, C. Attanasio, Eur. Phys. J. B **80**, 445 (2011).

[24] C. Peroz, C. Villard, Phys. Rev. B **72**, 014515 (2005).

[25] L. Parlato, R. Latempa, G. Peluso, G.P. Pepe, R. Cristiano, R. Sobolewski, Supercond. Sci. Technol. **18**, 1244 (2005).

Chapter 3

Long range proximity effect in Nb/Py/Nb trilayers

We report measurements of the temperature dependence of the parallel upper critical field, $H_{c2\parallel}(T)$, in proximity coupled Nb/Py/Nb trilayers in which the thickness of the Py layer, d_{Py}, changes from 20 nm up to 432 nm. When d_{Py} is in the range 150-250 nm a coupling between the two superconducting outer layers is observed with $H_{c2\parallel}(T)$ showing a linear behavior from T_c down to temperatures relatively far from the critical transition temperature. We believe that this is due to a long-range proximity effect generated by the inhomogeneous magnetization related to the presence of stripe domains of proper size in thick Py layers.

3.1 Introduction

The interplay between superconductivity and ferromagnetism can be effectively studied through the proximity effect which arises when a superconductor (S) comes in contact with a ferromagnet (F) in artificial S/F hybrids [1]. As confirmed by several experiments [2], in the case of spin-singlet superconductivity the pair wave function penetrates from the S- to the F-layer over a distance ξ_F which is typically of the order of few nanometers since, in the diffusive limit, $\xi_F = \sqrt{\hbar D_F/E_{ex}}$ (here D_F and E_{ex} are respectively the electron diffusivity and the exchange energy in the ferromagnet). However, it has been theoretically demonstrated that spin-triplet pairing of the Cooper pairs can give rise to a long-range penetration of the superconducting condensate in

the F-layer since electrons with parallel spins are only weakly affected by the exchange field [3]. Spin-triplet correlations are generated if the singlet Cooper pairs present in the conventional S-layer experience regions of inhomogeneous magnetization on the F-side of the hybrid within their coherence lengths ξ_S [3, 4]. Moreover, these pair correlations have even orbital angular momentum and are odd in frequency so they are robust against non-magnetic disorder [5]. Experimental evidence of the existence of long-range spin-triplet superconductivity has been recently reported [6].

In this Chapter, we investigate the temperature dependence of the parallel upper critical magnetic field, $H_{c2\parallel}(T)$, in unstructured S/F/S trilayers consisting of very well studied metallic materials, namely Nb/Py/Nb, where Nb and Py stand respectively for Niobium and Permalloy ($Ni_{80}Fe_{20}$). We show that when stripe domains (SDs) are induced [7–9] (for thickness of the Py layer starting at approximately 150 nm) the two outer Nb layers are coupled down to relatively high temperatures ($\approx 0.9\,T_c$, T_c is the superconducting critical temperature). We interpret this effect, which cannot be explained in terms of spin-singlet proximity theory, as due to long-range spin-triplet proximity effect generated by inhomogeneous magnetic patterns (noncollinear magnetization) [10] of very thick Py films.

3.2 Samples preparation and magnetic characterization

Nb/Py/Nb trilayers have been grown on Si(100) substrates by ultrahigh vacuum dc diode magnetron sputtering at room temperature. The deposition conditions are similar to those used to sputter similar S/F hybrids as described elsewhere [11]. The typical deposition rates are 0.25 nm/s for Nb and 0.30 nm/s for Py measured by a quartz crystal monitor previously calibrated by low-angle x-ray reflectivity measurements on deliberately deposited thin films of each material. Samples have constant Nb thickness, $d_{Nb} = 25$ nm, and variable Py thickness with d_{Py} in the range $20 - 432$ nm. For reference a single 25-nm-thick Nb film and several single Py films having the same thickness as the Py layers in the corresponding hybrids have also been prepared. All the samples are unstructured with typical in-plane dimensions of 50 mm^2. The transport properties have been measured in an in-line four-terminal geometry. The distance between the current (voltage) pads is about 0.8 cm (0.3 cm).

A detailed magnetic characterization of Py has been performed by measuring hysteresis cycles on the single Py films. All experiments have been performed in a commercial (Quantum Design) magnetometer. Figure 3.1 shows the complete hysteresis cycles measured at $T = 300$ K on the single 432-nm-thick Py film with the magnetic

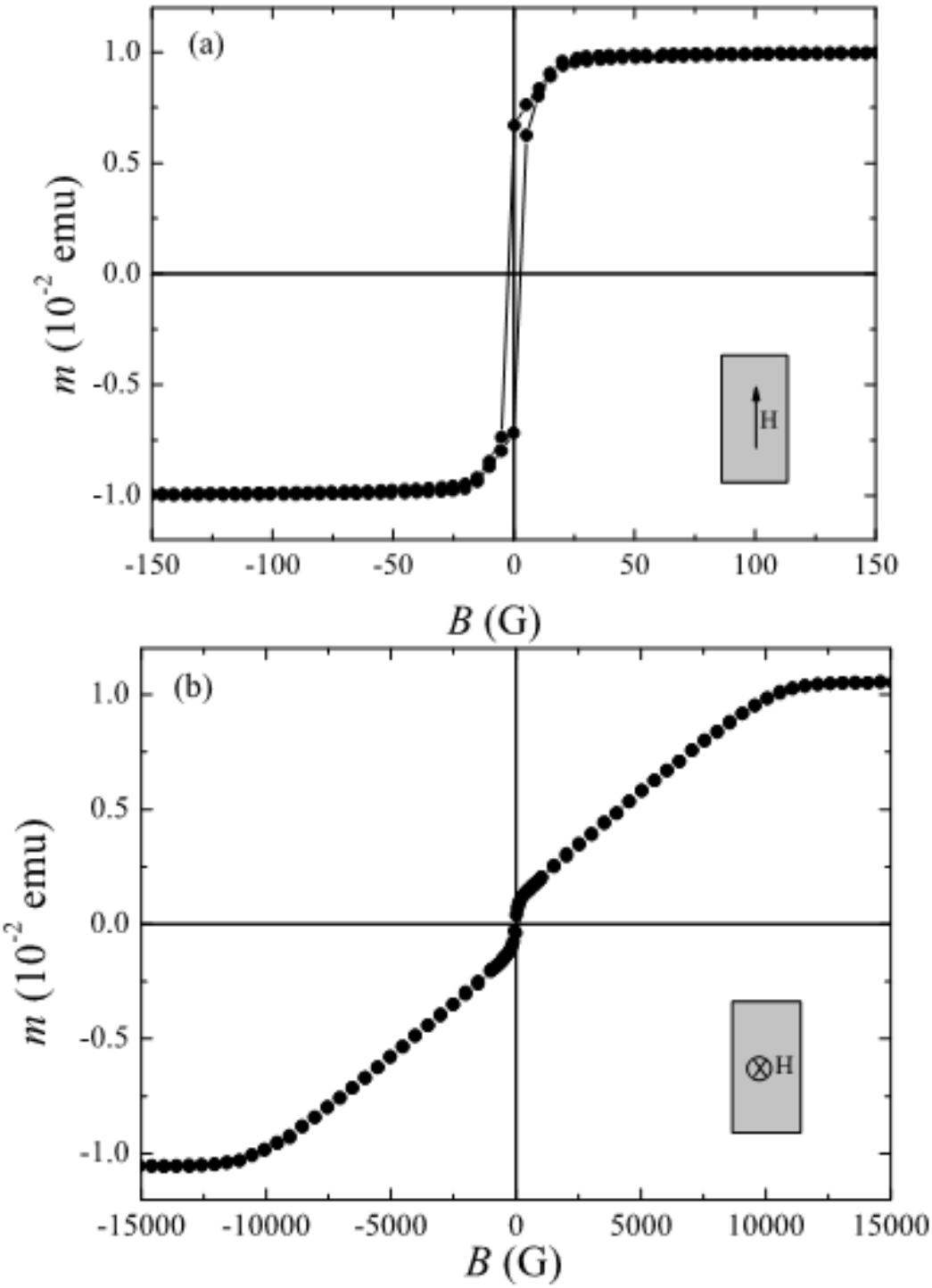

Figure 3.1: *Magnetic hysteresis cycle of the single 432-nm-thick Py film measured at $T = 300$ K with the applied magnetic field parallel (a) and perpendicular (b) to the substrate plane.*

field applied parallel (panel a) and perpendicular (panel b) to the substrate plane. The sample was first submitted to the application of a magnetic field of 1 T, which was subsequently removed prior to recording the hysteresis cycles. The characteristic

shape of the in-plane loop is a signature of the existence of a SD structure that appears in Py films above a certain critical thickness due to the formation of an out-of-plane magnetization component [12]. In this situation, the magnetization vector is parallel to the stripes in all domains but deviates alternately upward and downward from the plane of the film as a consequence of the presence of a negative magnetostriction constant that originates a weak perpendicular anisotropy [8, 13]. The critical thickness for the formation of SDs depends on fabrication conditions such as, for example, the deposition rate and the substrate temperature [7–9]. From the hysteresis cycles of Fig. 1 we may determine the saturation fields in the parallel and perpendicular directions to be respectively $H_{\parallel}^{\rm sat} \simeq 500$ Oe and $H_{\perp}^{\rm sat} \simeq 11800$ Oe. Using formulas for materials with small perpendicular anisotropy [14],

$$H_{\perp}^{\rm sat} = 4\pi M_s(1 - K_u/2\pi M_s^2), \quad H_{\parallel}^{\rm sat} = 2K_u/M_s, \tag{3.1}$$

the saturation magnetization and the uniaxial anisotropy constant were estimated to be respectively $M_s \simeq 980$ G and $K_u \simeq 2.44 \times 10^5$ erg/cm^3. Substituting in the expression for the critical thickness for the formation of the SD structure, $d_c = 2\pi(A/K_u)^{1/2}$ [7], the value obtained for K_u and the figure commonly cited for the exchange constant of Py, $A \simeq 1 \times 10^{-6}$ erg/cm [15], we obtain $d_c \simeq 125$ nm.

3.3 H-T phase diagrams

The H-T phase diagrams have been determined for all the trilayers by measuring the resistive transitions at fixed values of the external magnetic field. The latter has always been applied perpendicularly to the bias current and alternatively parallel ($\parallel$) or orthogonal ($\perp$) to the substrate plane. T_c has been defined at the 50% of the resistive transition curves. In zero field the width of the transitions, $T(R = 0.9R_n) - T(R = 0.1R_n)$ (R_n is the resistance at $T = 10$ K), is typically 50 mK for all the samples and this value does not substantially increase when the curves are measured in magnetic field. From the linear temperature dependence of the perpendicular upper critical fields (not reported here) the Ginzburg-Landau (GL) coherence length at zero temperature, $\xi_{GL}(0)$, has been extracted [16]. The values are around 10 nm for all the samples implying a superconducting coherence length $\xi_S(0) = (2/\pi)\xi_{GL}(0) \approx 7$ nm. The single Nb film, with $T_c = 6.5$ K, exhibits a two-dimensional (2D) behavior for the parallel upper critical field [17], $H_{c2\parallel}(T) \propto \sqrt{1 - T/T_c}$, in the entire investigated temperature range (measurement not shown here).

Figure 3.2 shows $H_{c2\parallel}(T)$ phase diagrams for a representative of Nb/Py/Nb trilayers. For all the hybrids we first apply at low temperature a strong magnetic field (approximately 1 T) in the plane of the samples and then we remove it. If the Py thickness is larger than d_c, magnetic SDs form in the direction of the applied field and remain fixed once the magnetic field has been reduced to zero [13, 18]. Starting from panel (a) in the figure, we observe that the sample Nb(25)/Py(105)/Nb(25) (numbers in parentheses indicate the thickness expressed in nm) exhibits a 2D-like behavior in the whole temperature range up to T_c. The black line is the square-root temperature dependence of $H_{c2\parallel}(T)$ obtained leaving $H_{c2\parallel}(0)$ as the only fitting parameter. If, due to the reduced Nb thickness, the Cooper pairs from both Nb layers do not penetrate deeply enough into the Py one, the temperature dependence of $H_{c2\parallel}$ should be 2D since the two Nb layers are decoupled [16]. Similar results, with a 2D behavior for $H_{c2\parallel}(T)$, have also been obtained for the thinnest sample, namely Nb(25)/Py(20)/Nb(25). This experimental evidence is not particularly surprising since decoupling of superconducting layers by ultrathin ferromagnetic ones were already observed in the literature on different S/F hybrids several years ago [19].

However, it is worth noticing that if the thickness of the inner Py layer is further increased, the 2D behavior is observed only until a certain temperature, the so-called 2D–3D crossover temperature, T_{cr}^{2D-3D}, above which the temperature dependence of the parallel upper critical field shows a three-dimensional (3D) behavior, $H_{c2\parallel}(T) \propto (1 - T/T_c)$ [17]. This result is reported in panels (b) and (c) of Figure 3.2 for the Nb(25)/Py(144)/Nb(25) and Nb(25)/Py(216)/Nb(25) trilayers, respectively. The insets in the panels show an enlargement of the data for temperatures close to T_c where the linear behavior of $H_{c2\parallel}(T)$ is much more evident since the two outer layers are coupled down to temperatures relatively far from T_c ($t \equiv T/T_c = 0.93$). Finally, if the Py thickness is increased above 250 nm, the 2D behavior is restored up to $T = T_c$ as reported in panel (d) of Figure 3.2, which refers to the Nb(25)/Py(432)/Nb(25) trilayer.

The previous analysis of the H-T phase diagrams is summarized in Figure 3.3 where the reduced crossover temperature ($t_{cr}^{2D-3D} \equiv T_{cr}^{2D-3D}/T_c$) is reported for all the trilayers (closed circles). For values of d_{Py} up to 100 nm (region A) and larger than 250 nm (region C) t_{cr}^{2D-3D} is essentially equal to 1 while in the range between 140 nm and 250 nm (region B) it is $t_{cr}^{2D-3D} = 0.93 - 0.95$. Samples lying in Region A are the ones in which the Py layers do not present magnetic stripes. This means that the two Nb layers feel a homogeneous magnetization and ξ_F dictates the penetration length of superconductivity in the inner F-layer. Since $D_F = (1/3)v_F\ell_F$, using $E_{ex} = 201$ meV, $v_F = 2.2 \times 10^5$ m/s [2, 20], and $\rho\ell_F = 31.5 \times 10^{-6}$ $\mu\Omega$ cm^2 [21], from the low-temperature values of the Py resistivity measured on our samples ($\rho = 20$ $\mu\Omega$ cm), we obtain $\xi_F \approx 1.9$ nm, a value which does not allow the coupling between the two external Nb layers. In fact, already for $d_{Py} = 20$ nm the order parameter is attenuated

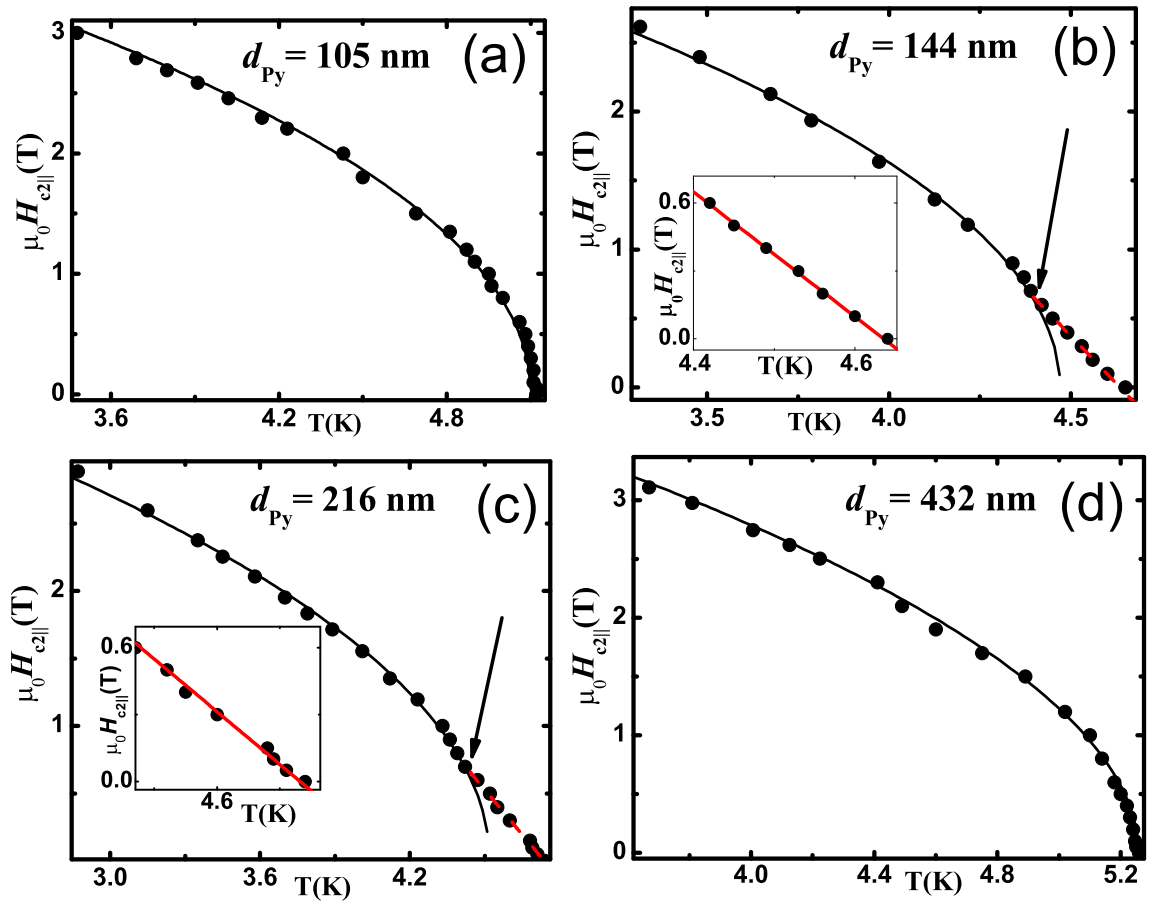

Figure 3.2: *Temperature dependence of the upper parallel critical field of Nb/Py/Nb trilayers with d_{Nb} = 25 nm and (a) d_{Py} = 105 nm, (b) d_{Py} = 144 nm, (c) d_{Py} = 216 nm, and (d) d_{Py} = 432 nm. Straight lines show the square-root temperature dependence of $H_{c2\|}$ valid for 2D superconductors obtained leaving as a fitting parameter only $H_{c2\|}(0)$. Dashed lines in (b) and (c) show the linear temperature dependence of $H_{c2\|}$ valid for 3D superconductors. The arrows show the temperature where the crossover between the 2D and the 3D regime takes place, T_{cr}^{2D-3D}. The insets of (b) and (c) show the high-temperature region of the respective H-T phase diagrams.*

at the center of the ferromagnetic layer by the factor $\exp(-d_{Py}/2\xi_F) = 5 \times 10^{-3}$, while for $d_{Py} = 100$ nm it is as small as $\exp(-d_{Py}/2\xi_F) = 3 \times 10^{-12}$.

On the other hand, for d_{Py} larger than 125 nm we know, from the magnetic characterization, that SDs form in the F-layer. In this case, if the Cooper pairs from the superconductor experience regions of noncollinear magnetization within their coherence lengths, ξ_S, long-range spin-triplet pair correlations may be generated [3]. In

agreement with theoretical works [5] which suggest that the non-homogeneous exchange field generated by the ferromagnetic domain walls could be a possible source of triplet pairing, we can define a crossover temperature, T_{cr}, as the temperature at which $\xi_S(T) = \xi_S(0)/\sqrt{1-T/T_c} \approx \delta_W$, where δ_W is the width of the Bloch walls connected to the presence of SDs in the Py layer. Since δ_W corresponds to a rotation of π of the magnetization between two adjacent stripes, we consider it as a measure of the region where the magnetization is inhomogeneous. Using the values obtained above for M_s and K_u, the stripe width can be estimated [14] as $w = (\pi d_{Py})^{1/2}[(1 + K_u/2\pi M_s^2)(A/K_u)]^{1/4} \simeq 8 d_{Py}^{1/2}$. Assuming that a reasonable value for δ_W should be about 1/3 of w, we can immediately determine the crossover temperature as $t_{cr}^{calc} \equiv T_{cr}^{calc}/T_c \simeq 1 - (6.9/d_{Py})$.

Open squares in Figure 3.3 represent the values for t_{cr}^{calc} estimated within our approximation. We can see that the above assumption satisfactorily reproduces the experimental data for t_{cr}^{2D-3D}. In region B t_{cr}^{calc} is lower than one, while if d_{Py} (and, consequently, δ_W) is further increased the calculated values for t_{cr}^{calc} tend to be again equal to one since the width of domain walls becomes too large for Nb to experience an inhomogeneous magnetization (region C). Of course, since $\xi_F \approx 1.9$ nm the long-range coupling in region B cannot be explained by singlet proximity effect. However, if spin-triplet superconductivity is established in the ferromagnet the penetration length of the Cooper pairs from both Nb layers into Py is determined by $\xi_F^T(T) = \sqrt{\hbar D_F/2\pi k_B T}$ [3], which can be much larger than ξ_F. In our case, we have $\xi_F^T(T = 4.2\text{ K}) \approx 20$ nm. Consequently, the order parameter for the sample with $d_{Py} = 144$ nm is attenuated at half the Py layer only by the factor $\exp(-d_{Py}/2\xi_F^T) = 3 \times 10^{-2}$ at 4.2 K and this explains why the two Nb layers feel each other despite the presence of the very thick ferromagnetic interlayer.

3.4 Enhancement of the critical temperature

In addition to the generation of spin-triplet superconductivity in Py, the presence of SDs in thick Py layers should also cause an enhancement of the superconducting critical temperature of the S/F/S systems with respect to the case of homogeneous magnetization in the F-layer. In this case, in fact, the pair-breaking mechanism produced by the exchange field becomes less effective at the domain walls, where the superconductivity is less strongly depressed [22]. Two resistive transitions for the Nb(25)/Py(432)/Nb(25) trilayer are shown in Figure 3.4. Open circles refer to the measurement performed just cooling the sample in zero field, while closed symbols

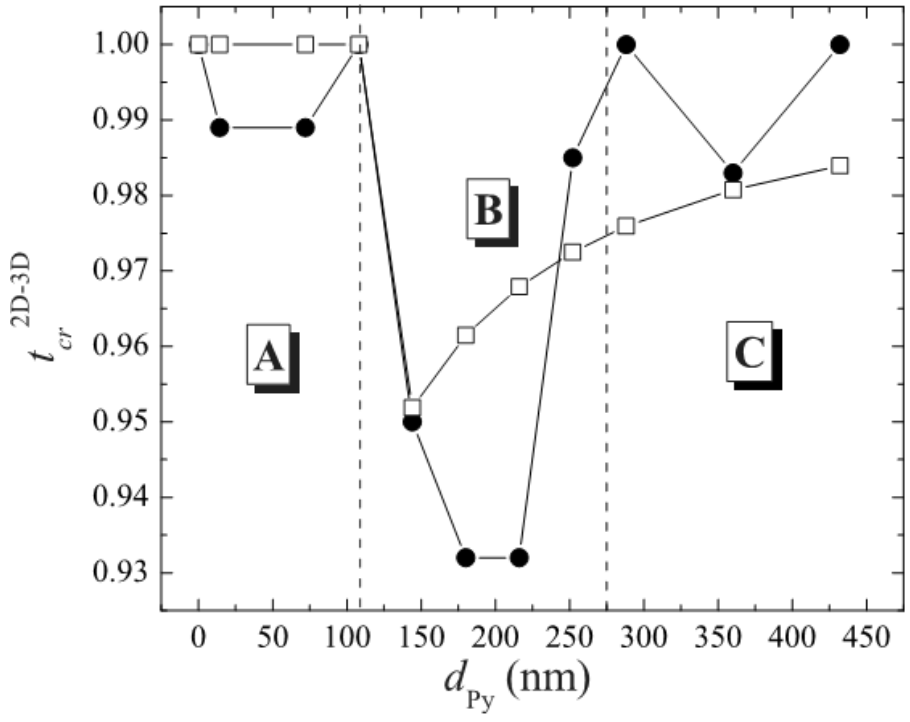

Figure 3.3: *Reduced 2D–3D crossover temperature as a function of the Py layer thickness in the Nb(25)/Py(x)/Nb(25) trilayers. Closed symbols represent experimental data while open symbols show the reduced crossover temperature calculated assuming* $\xi_S(t_{cr}^{calc}) = \delta_W$. *The dashed lines enclose the region of* d_{Py} *values for which the two Nb layers are coupled.*

represent the resistive transition in presence of SDs induced by first applying and then reducing to zero a strong in-plane magnetic field. If T_{cF} is the critical temperature when the superconductor is in contact with a homogeneous ferromagnet and T_{cW} is the critical temperature for the inhomogeneous case, the enhancement of the critical temperature defined as $\Delta T_c = T_{cW} - T_{cF}$ is relevant since $\Delta T_c = 30$ mK at half the resistive transitions. However, as reported in the inset of Figure 3.4, this effect is present only when the Py thickness (i.e. the domain wall widths) is in a suitable range of values. The so-called domain wall superconductivity is, in fact, observable only when $\delta_W \approx \xi_S$. An estimation for ΔT_c can be given following the theory developed in the case of domain-wall superconductivity in S/F proximity coupled systems [22]. Defining the relative increase of critical temperature as $\alpha \equiv \Delta T_c/T_{cF}$, and considering $\alpha \approx [\xi_S(0)/\delta_W]^2$ [22], if we take as a typical average value $\delta_W \approx 60$ nm and $T_{cF} \approx 5$ K for the samples where the shift in T_c is observed, we obtain $\Delta T_c \simeq 50$ mK in very good agreement with the experimental result.

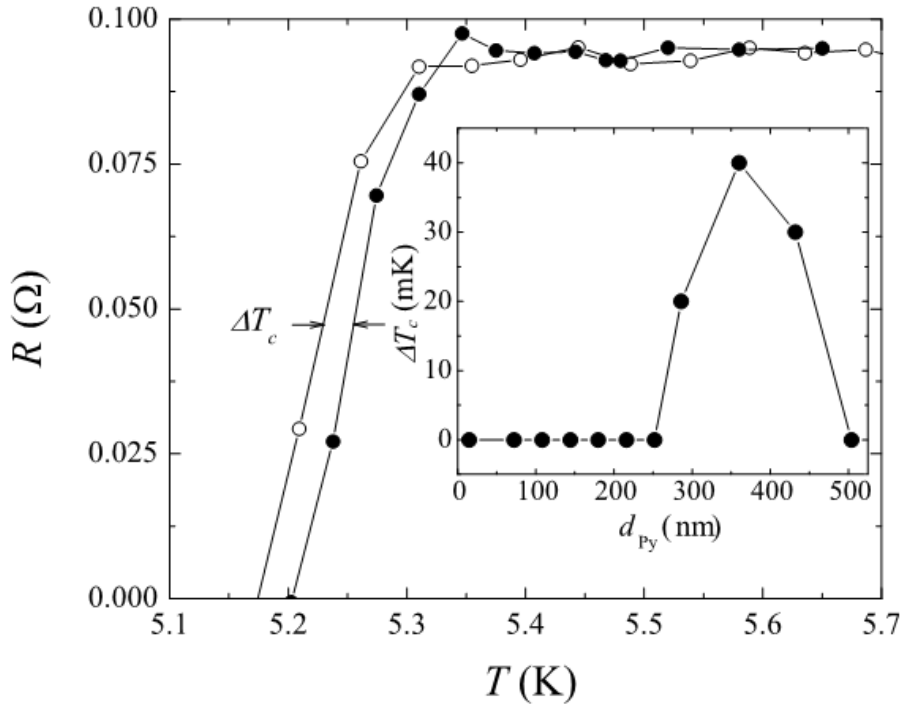

Figure 3.4: *Zero-field resistive transition for the Nb(25)/Py(432)/Nb(25) trilayer. Open (Closed) circles correspond to the measurement performed in presence (absence) of SDs in the Py layer. Inset: enhancement of the critical temperature due to presence of SDs in the F-layer as a function of* d_{Py}.

3.5 Conclusions

In conclusion, coupling between two Nb layers from T_c down to temperatures of $0.9\,T_c$ has been observed by parallel upper critical field measurements in very simple Nb/Py/Nb trilayers, when the thickness of the Py layer is in the range between 150 and 250 nm. This distance is much longer than the singlet decay length which is of the order of 2 nm in our Py film. The effect is related to the presence of stripe domain patterns in Py layers thicker than a certain critical value since such patterns produce a non-homogeneous magnetization which generates a long-range spin-triplet superconductivity in the system. When stripe domains are present the inhomogeneous magnetization of the Py layers also enhances significantly the critical temperature of the trilayers.

Bibliography

[1] A. A. Golubov, M. Yu. Kupriyanov, and E. Il'ichev, Rev. Mod. Phys. **76**, 411 (2004); A. I. Buzdin, Rev. Mod. Phys. **77**, 935 (2005).

[2] T. Kontos, M. Aprili, J. Lesueur, and X. Grison, Phys. Rev. Lett. **86**, 304 (2001); V. V. Ryazanov, V. A. Oboznov, A. Yu. Rusanov, A. V. Veretennikov, A. A. Golubov, and J. Aarts, Phys. Rev. Lett. **86**, 2427 (2001); J. W. A. Robinson, S. Piano, G. Burnell, C. Bell, and M. G. Blamire, Phys. Rev. Lett. **97**, 177003 (2006).

[3] F. S. Bergeret, A. F. Volkov, and K. B. Efetov, Phys. Rev. Lett. **86**, 4096 (2001).

[4] A. Kadigrobov, R. I. Shekhter, and M. Jonson, Europhys. Lett. **54**, 394 (2001).

[5] F. S. Bergeret, A. F. Volkov, and K. B. Efetov, Rev. Mod. Phys. **77**, 1321 (2005).

[6] I. Sosnin, H. Cho, V. T. Petrashov, and A. F. Volkov, Phys. Rev. Lett. **96**, 157002 (2006); R. S. Keizer, S. T. B. Goennenwein, T. M. Klapwijk, G. Miao, G. Xiao, and A. Gupta, Nature **439**, 825 (2006); T. S. Khaire, M. A. Khasawneh, W. P. Pratt, Jr., and N. O. Birge, Phys. Rev. Lett. **104**, 137002 (2010); M. S. Anwar, F. Czeschka, M. Hesselberth, M. Porcu, and J. Aarts, Phys. Rev. B **82**, 100501 (2010); J. W. A. Robinson, J. D. S. Witt, and M. G. Blamire, Science **329**, 59 (2010); M. S. Anwar, M. Veldhorst, A. Brinkman, and J. Aarts, arXiv:1111.5809v1.

[7] J. Ben Youssef, N. Vukadinovic, D. Billet, and M. Labrune, Phys. Rev. B **69**, 174402 (2004).

[8] N. Amos, R. Fernandez, R. Ikkawi, B. Lee, A. Lavrenov, A. Krichevsky, D. Litvinov, and S. Khizroev, J. Appl. Phys. **103**, 07E732 (2008).

[9] T. Dastagir, W. Xu, S. Sinha, H. Wu, Y. Cao, and H. Yu, Appl. Phys. Lett. **97**, 162506 (2010).

[10] M. Houzet and A. I. Buzdin, Phys. Rev. B **76**, 060504 (2007).

[11] C. Cirillo, E. A. Ilyina, and C. Attanasio, Supercond. Sci. Technol. **24**, 024017 (2011).

[12] N. Saito, H. Fujiwara, and Y. Sugita, J. Phys. Soc. Jpn. **19**, 421 (1964); **19**, 1116 (1964).

[13] A. Belkin, V. Novosad, M. Iavarone, J. Fedor, J. E. Pearson, A. Petrean-Troncalli, and G. Karapetrov, Appl. Phys. Lett. **93**, 072510 (2008).

[14] Y. Murayama, J. Phys. Soc. Jpn. **21**, 2253 (1966).

[15] B. B. Pant and K. Matsuyama, Jpn. J. Appl. Phys. Part 1 **32**, 3817 (1993).

[16] M. Schöck, C. Sürgers, and H. v. Löhneysen, Eur. Phys. J. B **14**, 1 (2000).

[17] C. S. L. Chun, G.-G. Zheng, J. L. Vincent, and I. K. Schuller, Phys. Rev. B **29**, 4915 (1984).

[18] V. V. Vlasko-Vlasov, U. Welp, G. Karapetrov, V. Novosad, D. Rosenmann, M. Iavarone, A. Belkin, and W.-K. Kwok, Phys. Rev. B **77**, 134518 (2008).

[19] P. Koorevaar, Y. Suzuki, R. Coehoorn, and J. Aarts, Phys. Rev. B **49**, 441 (1994); J. S. Jiang, D. Davidovic, D. H. Reich, and C. L. Chien, Phys. Rev. B **54**, 6119 (1996); G. Verbanck, C. D. Potter, V. Metlushko, R. Schad, V. V. Moshchalkov, and Y. Bruynseraede, Phys. Rev. B **57**, 6029 (1998).

[20] J. W. A. Robinson, S. Piano, G. Burnell, C. Bell, and M. G. Blamire, Phys. Rev. B **76**, 094522 (2007).

[21] A. F. Mayadas, J. F. Janak, and A. Gangulee, J. Appl. Phys. **45**, 2780 (1974).

[22] A. Yu. Rusanov, M. Hesselberth, J. Aarts, and A. I. Buzdin, Phys. Rev. Lett. **93**, 057002 (2004); M. Houzet and A. I. Buzdin, Phys. Rev. B **74**, 214507 (2006).

Chapter 4

Enhancement of T_C in Nb/Py/Nb trilayers

Superconducting critical temperature, T_c, have been measured in a Nb/Py/Nb series (here Py = $Ni_{80}Fe_{20}$) trilayers having constant Py thickness, $d_{Py} = 432$ nm, and variable Nb thickness, d_{Nb}, in the range $20 - 30$ nm. We have observed that, for d_{Nb} between 23 and 27 nm, resistive transitions shift towards higher temperature if stripe domains are present in the Py layer. We relate those observations to the non−homogeneous magnetization in the Py layer due to the presence of stripe domain structures.

4.1 Introduction

Superconducting (S) and Ferromagnetic (F) order parameters have an opposed nature and the problem of their mutual influence in thin films hybrids coupled by proximity effect has attracted a great attention [1, 2]. Such S/F heterostructures offer a variety of exciting new phenomena, which have been extensively discussed in recent years, such as the so-called spin triplet superconductivity [3]. Contrary to the case of conventional opposite spin pairing, where the proximity effect is short ranged, in the case of equal spin pairing the induced superconducting ordering penetrates deeply into the magnetic material and it is stable both in the dirty limit and the in presence of an exchange field. The triplet character of the long-ranged proximity effect can be generated in presence of an inhomogeneous magnetic ordering. Theoretical works

[3] suggest that the non-homogeneous exchange field generated by the ferromagnetic domain walls could be a possible source of spin triplet pairing. Indeed the effect of the domain walls on the superconducting properties of S/F hybrids has been experimentally investigated in systems made of strong as well as weak ferromagnets [4–7] and even in devices consisting of a single domain wall [8]. In particular, these works report on the domain wall induced critical temperature enhancement, in accordance with the theoretically estimations [9], on the increase of the critical current density, as well as on the magnetoresistance minima at the coercive fields, H_c. In all these experiments it is extremely important to rule out all the possible effects arising from undesired stray fields proliferating at H_c. This problem has been deeply investigated in Ref. [10].

In this Chapter we study the influence of the magnetic domain structure of thick Permalloy (Py = $Ni_{80}Fe_{20}$) layer on thin Nb films in Nb/Py/Nb trilayers, showing that the presence of the peculiar stripe domain structure provides an enhancement of the critical temperature of the samples.

4.2 Experiment

Nb/Py/Nb trilayers have been deposited on Si(100) substrates by UHV dc diode magnetron sputtering at room temperature, at a base pressure of 2×10^{-8} Torr and at processing Ar pressure of 3×10^{-3} Torr. The typical deposition rates were 0.25 nm s^{-1} for Nb and 0.3 nm s^{-1} for Py, as measured by a quartz crystal monitor previously calibrated by low-angle X-ray reflectivity measurements on deliberately deposited thin films of each material. Samples have an internal Py layer of constant thickness (d_{Py} = 432 nm) and varying external Nb layers thicknesses (d_{Nb} = 20 - 30 nm). For reference a single Py films, 432 nm thick, used for magnetic characterization, has also been prepared.

Among ferromagnetic materials, Py has a high magnetic permeability, low coercivity, and near zero magnetostriction. Usually Py thin films have in-plane shape anisotropy. However, for films thicker than some critical thickness, d_{Py}^{cr}, an out-of-plane magnetization component could be formed. Consequently, an array of alternating adjacent magnetic domains, known as stripe domains, (SDs), often forms. The critical thickness at which the SDs appears varies depending on deposition conditions [11–13]. In our case an approximate value of the critical Py thickness for the SDs formation is 150-200 nm. All the samples were unstructured with typical in-plane dimensions of 50 mm^2. The measurements have been performed using a standard four-contact configuration. The values of the critical temperatures T_c have been extracted from the $R(T)$ curves taking the 50% value of the normal state resistance R_N just above the transition to the superconducting state. From upper critical magnetic field measure-

ments a value of $\xi_{GL}(0) \approx 10$ nm has been estimated for the superconducting layer. For inducing SDs in the Py layers for all the hybrids we first apply at $T = 4.2$ K a strong magnetic field (approximately 1 T) in the plane of the samples and then we remove it. If the Py layer is thicker than d_{Py}^{cr}, SDs are formed, persisting also after reducing the in-plane field to zero [14, 15].

4.3 Results and discussion

A detailed magnetic characterization has been performed on the single Py film with the same thickness used in the trilayers ($d_{Py} = 432$ nm). The measurements have been realized using a commercial Quantum Design Magnetic Properties Measurement System magnetometer. In Figure 4.1 the magnetization curves, $m(B)$, measured at $T = 300$ K with the magnetic field applied (a) parallel ($\parallel$) and (b) perpendicular ($\perp$) to the sample plane are shown. The samples are characterized by a saturation magnetization of $M_s \approx 800$ emu/cm^3. Moreover, as one can see, hysteresis loops show the peculiar dependence of a film presenting the stripe domain structure [15].

Figure 4.1 confirms that the Py embedded in the analyzed Nb/Py/Nb trilayers presents a non-homogeneous magnetization caused by the presence of the SDs. According to the literature the period of the SD pattern is comparable with the film thickness [15]. Moreover the dimensions of the domain wall width separating the stripes can be estimated to be of the order of $\delta_w \approx 300$ nm [16].

δ_w plays an important role in the study of domain wall superconductivity [5, 9]. It represents the boundary between different magnetization orientations thus, at the wall, Cooper pairs experience a lower exchange field and this leads to a weaker suppression of superconducting ordering. Therefore the value of the domain wall width is crucial and it should be compared to the value of the superconducting coherence length, $\xi_S = 2\xi_{GL}/\pi$. If the size of the domain wall is much larger than ξ_S, in fact, the Cooper pairs will feel an uniform exchange field, and no effect will be observed. Indeed, it has been shown that the maximum effect for the domain wall superconductivity is obtained in the range $\delta_w \approx \xi_S$ [1]. In figure 4.2 two resistive transitions for the sample Nb(23 nm)/Py/Nb(23 nm) are reported. The blue curve refers to the transition measured on the virgin sample (where no SDs are present), while the red one indicates the measurement performed after first applying a strong in plane magnetic field ($\mu_0 H = 1$ T) in order to induce the SDs, and then removing it. A shift in the critical temperatures with $\Delta T_c = T_{c,SD}$ - $T_{c,noSD} \approx 30$ mK is evident. We believe that the presence of this pronounced effect, clearly related to the Py domain state, may be realized at $T \simeq T_c$ where, according to the temperature dependence $\xi_S(T) = \xi_S(0)(1 - T/T_c)^{-1/2}$, the

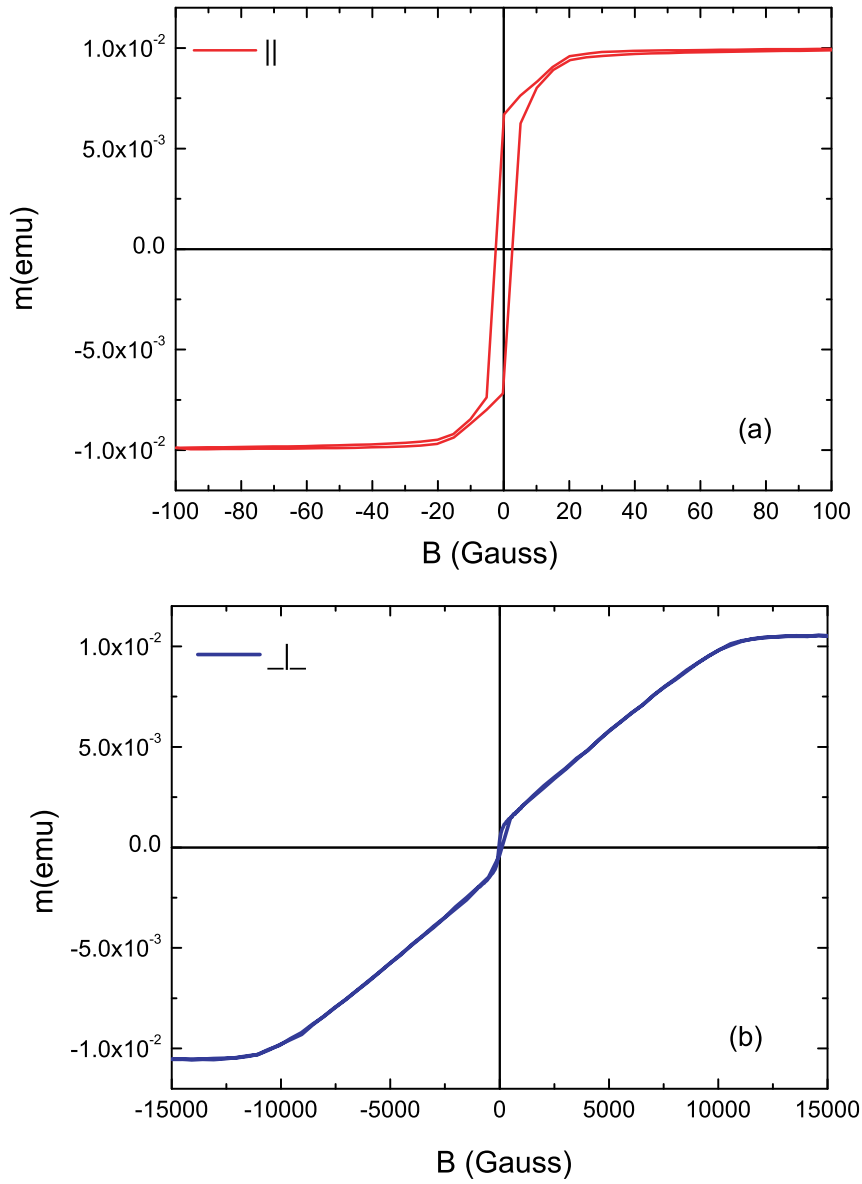

Figure 4.1: *Hysteresis loop of the single Py film 432 nm thick recorded at 300 K with the magnetic field applied (a) parallel (∥) and (b) perpendicular (⊥) to the plane of the substrate.*

condition $\delta_w \approx \xi_S(T)$ can be fulfilled.

The same experiment has been performed on different trilayers with equal Nb thickness but with $d_{Py} < d_{Py}^{cr}$, namely in the case where there is no SDs formation in the Py layer. In all these measurements we could not observe any shift of the critical temperature.

The study of the critical temperature enhancement has been systematically performed as a function of the Nb thickness as well. In figure 4.3 the dependence of $\Delta T_c(d_{Nb})$ curve is reported (left scale), together with dependence of the critical temperature in the virgin state, $T_{c,noSD}$, on d_{Nb} (right scale). The T_c shift is clearly present

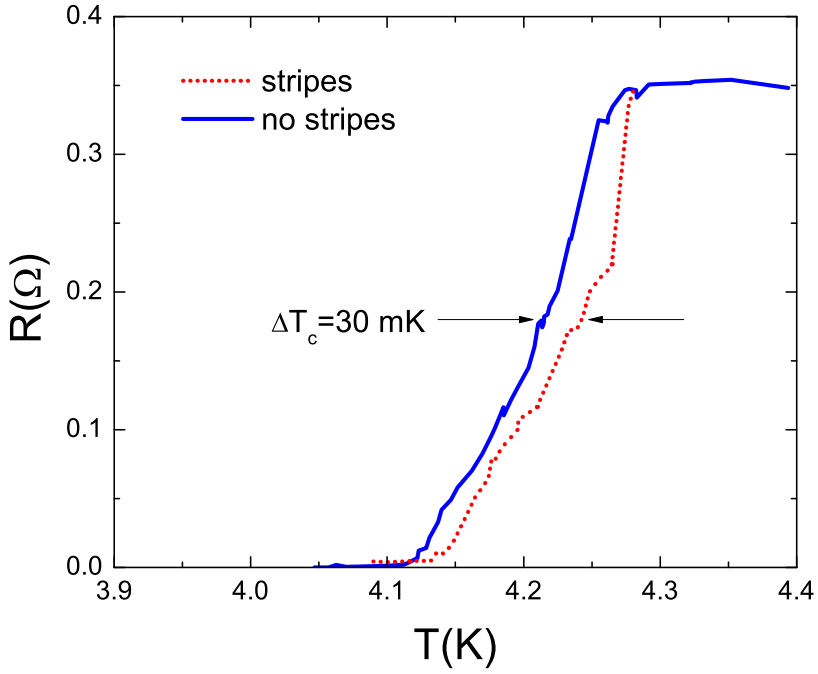

Figure 4.2: *Resistive transitions for the trilayer with d_{Nb} = 23 nm. Straight (dotted) curve refers to the measurement performed on the sample without (with) SDs in the Py layer.*

for Nb thickness in the region from 23 up to 27 nm. To interpret this result is again necessary to take into account the value of $\xi_S(0)$, this time comparing it to the value of d_{Nb}. The superconducting layer is, in fact, sensitive to the influence of the ferromagnetic layer if a large fraction of d_{Nb} is involved into the proximity effect, namely if $d_{Nb} \approx \xi_S(0)$. Indeed, if d_{Nb} is roughly more than twice the superconducting coherence length, then it may be too thick to be affected by the domain configuration. Therefore this requirement on the d_{Nb} thickness is crucial for the observation of the peculiar phenomena typical of S/F structures, such as, for instance, non-monotonic $T_c(d_F)$ dependence [17–19], or spin-switch effect [20, 21]. For the sample presenting the T_c shift, in fact, it is: $1.15 \leq d_{Nb}/2\xi_S(0) \leq 1.35$. On the other hand, decreasing the Nb thickness down to $d_{Nb} = 20$ nm leads to a significant suppression of the superconducting ordering, as it can be inferred from the value of the critical temperature ($T_c = 4.17$ K), which is suppressed of the 20 percent compared to the sample with d_{Nb}= 30 nm ($T_c = 5.19$ K).

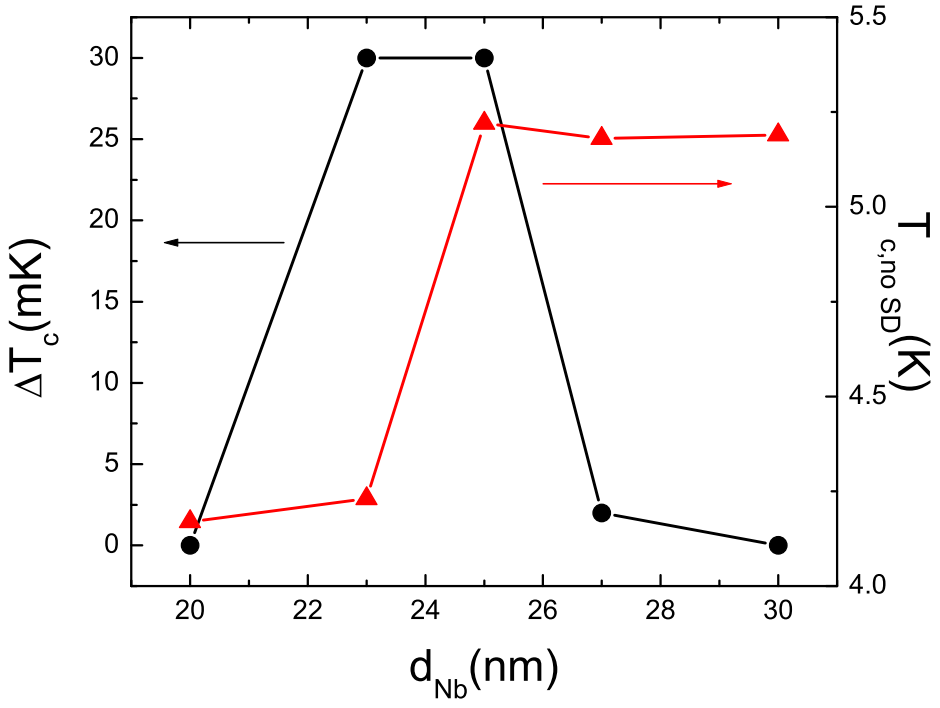

Figure 4.3: *(Left scale) Dependence of the shift of the critical temperature, ΔT_c=$T_{c,SD}$ - $T_{c,noSD}$, as a function of the Nb thickness, d_{Nb}. (Right scale) Critical temperature in the virgin state, $T_{c,noSD}$, as a function of d_{Nb}.*

4.4 Conclusions

We study the effect of the domain configuration of a thick Py film embedded in Nb/Py/Nb trilayers on the transition temperatures of these structures. A clear enhancement of T_c is observed when stripe domains are present in the ferromagnetic layer compared to the case where the latter is in its virgin state. The Nb thickness range in which this effect is present is discussed.

Bibliography

[1] A. I. Buzdin, Rev. Mod. Phys. **77**, 935 (2005).

[2] F. S. Bergeret, A. F. Volkov, and K. B. Efetov, Rev. Mod. Phys. **77**, 001321 (2005).

[3] A. F. Volkov, F. S. Bergeret, and K. B. Efetov, Phys. Rev. Lett. **90**, 117006 (2003).

[4] R. J. Kinsey, G. Burnell, and M. G. Blamire, IEEE Trans. Appl. Supercond. **11**, 904 (2001).

[5] A. Rusanov, M. B. S. Hesselberth, J. Aarts, and A.I. Buzdin, Phys. Rev. Lett. **93**, 57002 (2004).

[6] A. Rusanov, M. Hesselberth, S. Habraken, and J. Aarts, Physica C **404**, 322 (2004).

[7] M. Flokstra and J. Aarts, Phys. Rev. B **80**, 144513 (2009).

[8] A. S. Jenkins, S. Lepadatu, C. H. Marrows, and G. Burnell, J. Supercond. Nov. Magn. **24**, 911 (2011).

[9] M. Houzet and A. I. Buzdin, Phys. Rev. B **74**, 214507 (2006).

[10] E. J. Patiño, C. Bell, and M. G. Blamire, Eur. Phys. J. B **68**, 73 (2009).

[11] J. Ben Youssef, N. Vukadinovic, D. Billet and M. Labrune, Phys. Rev. B **69**, 174402 (2006).

[12] N. Amos, R. Fernandez, R. Ikkawi, B. Lee, A. Lavrenov, A. Krichevsky, D. Litvinov, and S. Khizroev, J. Appl. Phys. **103**, 07E732 (2008).

[13] T. Dastagir, W. Xu, S. Sinha, H. Wu, Y. Cao, and H. Yua, Appl. Phys. Lett. **97**, 162506 (2010).

[14] A. Belkin, V. Novosad, M. Iavarone, J. Fedor, J. E. Pearson, A. Petrean-Troncalli, and G. Karapetrov, Appl. Phys. Lett. **93**, 072510 (2008).

[15] V. V. Vlasko-Vlasov, U. Welp, G. Karapetrov, V. Novosad, D. Rosenmann, M. Iavarone, A. Belkin, and W.-K. Kwok, Phys. Rev. B **77**, 134518 (2008).

[16] T. Trunk, M. Redjdal, A. Kakay, M. F. Ruane, and F. B. Humphrey, J. Appl. Phys. **89**, 7606 (2001).

[17] Z. Radovic, M. Ledvij, L. Dobrosavljevic-Grujic, A. I. Buzdin, and J. R. Clem, Phys. Rev. B **44**, 759 (1991).

[18] L. R. Tagirov, Physica C **307**, 145 (1998).

[19] V. Zdravkov, A. Sidorenko, G. Obermeier, S. Gsell, M. Schreck, C. Müller, S. Horn, R. Tidecks, and L. R. Tagirov, Phys. Rev. Lett. **97**, 057004 (2006).

[20] I. C. Moraru, W. P. Pratt Jr., and N. O. Birge, Phys. Rev. B **74**, 220507 (2006).

[21] P. V. Leksin, N. N. Garifyanov, I. A. Garifullin, J. Schumann, V. Kataev, O. G. Schmidt, and B. Büchner, Phys. Rev. Lett. **106**, 067005 (2011).

Conclusions

In this thesis the S/F proximity effect has been studied in different Nb−based layered structures. In particular, when using a weakly ferromagnetic alloy, such as PdNi and CuNi, the dynamic instabilities of the vortex lattice at high driving currents have been measured and the role played on the non−equilibrium properties of the hybrids by the ferromagnetic material has been analyzed with a special focus on the values and the temperature dependence of the quasiparticle relaxation times, τ_E. The study revealed that the presence of the F-layer causes a reduction of τ_E, result that makes S/F hybrids extremely promising in the field of ultrafast superconducting single photon detectors. Moreover, we show that the nature of the ferromagnet coupled to the superconducting layer determines the dominant relaxation mechanisms of the systems. In fact, the use of a weak ferromagnet could be more suited to changing and tailoring the optical properties of the whole system. In particular, an increased electron−phonon interaction could reflect itself in an almost constant value of τ_E, a feature that could also be important in view of possible applications. Moreover, in the second part of the thesis a slightly different argument has been tackled namely the possibility to induce long range triplet superconductivity in Nb layers due to the presence of inhomogeneous magnetization in thick Py films (of the order of 200 nm). In particular, by measuring the temperature dependence of the parallel upper critical field, we have observed a coupling between the two Nb outer layers in Nb/Py/Nb trilayers. The distance over which the superconducting layers feel each other is two order of magnitude greater than the singlet decay length in Py films. The effect was related to the presence of stripe domain patterns in Py layers thicker than a certain critical value since such patterns produce a non−homogeneous magnetization which generates a long−range spin−triplet superconductivity in the system. When stripe domains are present the inhomogeneous magnetization of the Py layers also enhances the critical temperature of the trilayers.

Publications

1. **E.A.Ilyina**, C. Cirillo, C. Attanasio."I-V characteristics and critical currents in superconducting/ferromagnetic bilayers". Physica C **470**: 877-879 (2010).

2. **E.A.Ilyina**, C. Cirillo, C. Attanasio. "Quasiparticles relaxation processes in Nb/CuNi bilayers". European Physical Journal B, **83**: 53-56 (2011).

3. C. Cirillo, **E.A.Ilyina**, C. Attanasio. "Static and dynamic properties of the vortex lattice in superconductor/weak ferromagnet bilayers". Supercond. Sci. Technol. **24**: 024017 (8pp) (2011).

4. D. Mancusi, **E.A.Ilyina**, V.N. Kushnir, S.L. Prischepa, C. Cirillo, and C. Attanasio. "Evaluation of the specific boundary resistance of superconducting/weakly ferromagnetic hybrids by critical temperature measurements". Journal of Applied Physics **110**, 113904 (2011).

5. **E.A.Ilyina**, J. M. Hernandez, A. Garcìa-Santiago, C. Cirillo, C. Attanasio. "Enhancement of the superconducting critical temperature in Nb/Py/Nb trilayers". Accepted for publication in Physica C, availiable online (2011).

6. K. Torokhtii, C. Attanasio, C. Cirillo, **E.A.Ilyina**, C. Meneghini, N. Pompeo, S. Sarti, E. Silva. "Vortex motion in Nb/PdNi/Nb trilayers: new aspects in the flux flow state". Accepted for publication in Physica C (2011).

7. **E.A.Ilyina**, C. Cirillo, J. M. Hernandez, A. Garcìa-Santiago, J. Tejada, and C. Attanasio. "Effect of inhomogeneous magnetization on the superconducting properties of Nb/Py/Nb trilayers: evidence of spin-triplet superconductivity". Submitted.

Acknowledgements

At the end of my work time, it is a pleasure for me to write some words of gratitude to all who made this thesis possible.

First and foremost, I want to thank my advisor Prof. Carmine Attanasio for giving me the opportunity to work in his group during my entire Ph.D program. Prof. Attanasio has supported me throughout my thesis with his expertise, his understanding, his patience and his knowledge. One simply could not wish for a better or friendlier supervisor!

A big thanks to Prof. Serghej Prischepa, who guided me along my first steps in research. With his enthusiasm, his inspiration, and his great efforts to explain things clearly and simply, he helped to make physics fun for me.

I have been blessed with such a friendly and cheerful group of talented people to work with. I am very grateful to Dr. Carla Cirillo for her invaluable assistance and support in the laboratory and very kind help with all official Italian matters.

I would like to thank Michela Trezza for sharing studying hours in our office, for her encouragement and the attention she has given me. And of course for her willingness to help anytime it was needed.

I also want to thank Davide Mancusi for sharing working time in the laboratory. Special thanks goes to the "MUSA" girls (Anita Guarino, Rosalba Fittipaldi and Veronica Granata) for the fun lunch time and useful tips about Italian life.

And a very special thanks I want to give to my dear family, my parents and my brother Pavel, for their love and constant support during my work.

Grazie mille a tutti!